



T.C

**YEDİTEPE UNIVERSITY**  
**THE INSTITUTE OF GRADUATE STUDIES IN SCIENCE&ENGINEERING**  
**MECHANICAL ENGINEERING**

**OPTIMIZATION OF THE BLOOD FLOW THROUGH A LEFT VENTRICULAR  
ASSIST DEVICE**

by

**A. Serhan HAKKOYMAZ**

**Submitted to the Institute of Graduate Studies in Science & Engineering  
in partial fulfillment of the requirements for the degree of  
Master of Science  
in Mechanical Engineering**

**ISTANBUL, 2008**

ISTANBUL  
2008



**T.C.  
YEDİTEPE UNIVERSITY  
THE INSTITUTE OF GRADUATE STUDIES IN SCIENCE&ENGINEERING  
MECHANICAL ENGINEERING**

**OPTIMIZATION OF THE BLOOD FLOW THROUGH A LEFT VENTRICULAR  
ASSIST DEVICE**

**by**

**A. Serhan HAKKOYMAZ**

**Supervisor  
Asst Prof. Dr. Esra SORGUVEN**

**Submitted to the Institute of Graduate Studies in Science & Engineering  
in partial fulfillment of the requirements for the degree of  
Master of Science  
in Mechanical Engineering**

**ISTANBUL, 2008**

**OPTIMIZATION OF THE BLOOD FLOW THROUGH A LEFT VENTRICULAR  
ASSIST DEVICE**

**by**

**A. SERHAN HAKKOYMAZ**

Approved by:

Yrd. Doç. Dr. Esra SORGUVEN  
(Supervisor)

.....

Prof. Dr. Nilüfer EĞRİCAN

.....

Yrd. Doç. Dr. Levent KAVURMACIOĞLU

.....

Date of Approval by the Administrative Council of the Institute 08/08/2008

## **ACKNOWLEDGEMENT**

I wish to express my appreciation to Asst. Prof. Esra SORGUVEN for her continuous support, guidance and encouragement during my thesis study. I would also like to thank Prof. Dr. Nilüfer EĞRİCAN for her support.

I would like to thank TUBITAK for their support. I also would like to thank honorable people of Yeditepe University Mechanical Engineering Department for their support and friendship.

I would like to express my special thanks to Cankat ERDOĞAN and Kıvılcım Eren ATEŞ for their encouragement.

Finally I would like to thank my family for their invaluable support.

## TABLE OF CONTENTS

<b>LIST OF SYMBOLS</b> .....	<b>i</b>
<b>LIST OF ABBREVIATIONS</b> .....	<b>ii</b>
<b>LIST OF FIGURES</b> .....	<b>iii</b>
<b>LIST OF TABLES</b> .....	<b>v</b>
<b>ABSTRACT</b> .....	<b>vi</b>
<b>ÖZET</b> .....	<b>vii</b>
<b>1 Introduction</b> .....	<b>1</b>
<b>2 Theory</b> .....	<b>3</b>
2.1 Physiologic System .....	3
2.1.1 Circulatory System .....	3
2.1.2 Blood .....	3
2.1.3 Blood Vessels .....	3
2.1.4 Heart .....	4
2.1.5 Circulation .....	4
2.1.6 Cardiac Failure .....	5
2.1.7 Mechanical Solutions .....	6
2.1.8 History .....	6
2.1.9 Blood Pumps .....	7
2.1.10 Complications .....	12
2.2 Design of an Axial Blood Pump .....	13
2.2.1 Velocity Components in a Rotating Domain .....	13
2.2.2 The Euler Turbomachinery Equation .....	14
2.2.3 Velocity Triangle .....	15
<b>3 Design and CFD</b> .....	<b>16</b>
3.1 Introduction .....	16
3.2 Micromed DeBakey LVAD .....	21
3.2.1 Simulation Results of the MicroMed DeBakey LVAD .....	22
3.3 Optimization .....	25
3.3.1 Simulation Results of the Optimization .....	25
3.4 Axial Pump With Arc-Shaped Blades .....	28
3.4.1 Impeller Geometry .....	28
3.4.2 Diffuser Geometry .....	29
3.4.3 Simulation Results of Arc Geometry .....	31
3.5 Axial Pump With Constant Pressure Increase Through The Blades .....	34
3.5.1 Calculations .....	34
3.5.2 Solid Modeling .....	40
3.5.3 Modifications .....	43
3.5.4 Simulation Results of Modification Models .....	45
3.5.5 Simulation Results of the 3. Modification .....	47
3.6 Results .....	49
<b>4 Discussion</b> .....	<b>52</b>

## LIST OF SYMBOLS

$V_a$	Axial velocity
$V_r$	Radial velocity
$V_\theta$	Tangential velocity
$\tau$	Torque
$m$	Mass flow rate
$r$	Radius
$w$	Angular speed
$U$	Blade speed
$H$	Enthalpy
$W_x$	Total shaft work per unit mass of fluid
$W$	Relative velocity
$W_\theta$	Tangential component of relative velocity
$W_a$	Axial component of relative velocity
$C$	Absolute velocity
$C_\theta$	Tangential component of absolute velocity
$C_a$	Axial component of absolute velocity
$N$	Rotor speed
$A$	Area
$\rho$	Density
Re	Reynolds number
$u$	Free stream velocity
$d$	Diameter
$\nu$	Dynamic viscosity
$\alpha$	Inlet angle of blade
$\lambda$	Degree of reaction

## **LIST OF ABBREVIATIONS**

LVAD	Left Ventricular Assist Device
CFD	Computational Fluid Dynamics
WSS	Wall Shear Stress



## LIST OF FIGURES

Figure 2.1: A Basic Table of Circulation.....	3
Figure 2.2: Heart and Circulation .....	5
Figure 2.3: Classification of Blood Pumps.....	7
Figure 2.4: The Liotta total artificial heart, the first one implanted in a human.....	8
Figure 2.5 Heartmate LVAD .....	9
Figure 2.6: MicroMed DeBakey ventricular assist device. ....	10
Figure 2.7: Levacor Ventricular Assist Device .....	11
Figure 2.8: PediPump assist device. ....	12
Figure 2.9: Velocities at any point of the pump .....	14
Figure 2.10: Velocity vectors of flow .....	15
Figure 3.1: Velocity changes through the impeller and diffuser. ....	18
Figure 3.2: Computational Mesh .....	20
Figure 3.3: Computational Domain .....	20
Figure 3.4: Micromed DeBakey’s solid model.....	21
Figure 3.5: Pressure distribution of DeBakey model.....	22
Figure 3.6: WSS distribution of DeBakey model .....	23
Figure 3.7: Relative velocity vectors of the DeBakey model .....	23
Figure 3.8: Relative velocity vectors around the splitter blades of DeBakey model.....	24
Figure 3.9: Absolute velocity vectors around the diffuser.....	25
Figure 3.10: Pressure Distribution of the Optimum .....	26
Figure 3.11: WSS Distribution of the Optimum.....	26
Figure 3.12: Relative Velocity Vectors of the Optimum.....	27
Figure 3.13: Absolute Velocity Vectors of the Optimum.....	27
Figure 3.14: Arc creation .....	28
Figure 3.15: Wrap around the cylinder and blade creation by arc.....	29
Figure 3.16: Impeller geometry designed by arc .....	29
Figure 3.17 : Diffuser geometry which is designed by using arc .....	30
Figure 3.18: Modified diffuser geometry which is designed by using arc. ....	31
Figure 3.19: Pump model designed by arc .....	31
Figure 3.20: Pressure distribution of the arc model.....	32
Figure 3.21: WSS distribution of the arc model .....	32
Figure 3.22: Relative velocity vectors of the arc models impeller .....	33
Figure 3.23: Absolute velocity vectors of arc models diffuser.....	33
Figure 3.24: Blade Speed Calculation .....	35
Figure 3.25: Calculation of the inlet angle .....	37
Figure 3.26: The flow area in axial direction.....	38
Figure 3.27: Section lengths in axial and tangential directions. ....	41
Figure 3.28: Spline creation.....	42
Figure 3.29: Wrap around the cylinder .....	42
Figure 3.30: Blade creation by spline .....	42

Figure 3.31: Impeller blades created by spline .....	43
Figure 3.32: 1. Modification model (impeller) .....	44
Figure 3.33: 2. Modification model (impeller) .....	45
Figure 3.34: 3. Modification model (impeller) .....	45
Figure 3.35: Comparison of pressure rises .....	46
Figure 3.36: Comparison of wall shear stresses .....	47
Figure 3.37: Pressure distribution of the 3. modification .....	48
Figure 3.38: WSS distribution of the 3. modification.....	48
Figure 3.39: Relative velocity vectors of 3. modification .....	49
Figure 3.40: General comparison of pressure rises.....	50
Figure 3.41: General comparison of WSS .....	51
Figure 3.42: Characteristic curve of the 3. modification model .....	51
Figure 3.43: WSS rates of the 3. modification model for different mass flow rates .....	52

## LIST OF TABLES

Table 1: Causes of death in the United States of America (2002) and Germany (2004) .....	5
Table 2: Pressure difference results for different blade speeds. ....	36
Table 3: Inlet and outlet angles of each section. ....	39
Table 4: Change of relative and absolute tangential velocities through the sections. ....	40
Table 5: Blade lengths of modified models .....	44
Table 6: Pressure rises and wall shear stresses .....	46
Table 7: Pressure rise and WSS levels of 3. modification model at different rpms. ....	50

## ABSTRACT

Cardiac failure is a frequently seen health problem which causes millions of deaths every year. The idea of supporting a failed heart until the transplantation via a mechanical system has been established with the developments in technology and medical science.

The aim of this thesis is to design an axial left ventricular assist device, which provides the necessary blood flux without damaging the blood cells. Thus, different axial blood pump models are designed and numerically investigated.

The first investigated model is the MicroMed DeBakey left ventricular assist device, which is one of the mostly preferred axial blood pumps in the clinical setting and chosen as the baseline design for this study. At the second step, an optimization study model, which was generated by using the parametric design method, is investigated. Third design is generated with arc shaped blades. At the fourth design, a linear increase in pressure across the blades is aimed. The blades are divided into ten equal sections in axial direction and the blade camber is computed with the help of the Euler turbomachinery equations.

Each pump model is investigated via the computational fluid dynamics. Pressure generation and blood damage rates are compared. The simulation results shows that the fourth model provides a %38 higher pressure rise with a %6 lower wall shear stress level than the MicroMed DeBakey LVAD.

## ÖZET

Kalp yetmezliđi sıklıkla görülen ve her sene milyonlarca insanın ölümüne yol açan bir sađlık sorunudur. Teknoloji ve tıp bilimindeki ilerlemelerle birlikte, hasta bir kalbin mekanik bir sistem vasıtasıyla desteklenmesi fikri ortaya çıkmıştır.

Bu tezin amacı, gerekli kan akışını kan hücrelerinde herhangi bir bozulmaya sebebiyet vermeden sağlayabilecek bir eksenel sol ventriküle destek cihazı tasarlamaktır. Bu amaçla, farklı eksenel kan pompaları tasarlanmış ve sayısal olarak incelenmiştir.

İlk olarak, klinik ortamda sıklıkla tercih edilen eksenel kan pompalarından birisi olan MicroMed DeBakey sol ventriküle destek cihazı, çalışmanın geneli için referans model olarak seçilmiş ve incelenmiştir. İkinci adımda ise, bir optimizasyon çalışmasında parametrik dizayn yöntemi ile oluşturulmuş bir model incelendi. Üçüncü tasarım ise yay şeklindeki kanatlardan oluşturuldu. Dördüncü tasarımda ise, kanat boyunca doğrusal bir basınç artış miktarı amaçlandı. Kanatlar eksenel yönde eşit uzunluklara sahip on parçaya bölündü ve kanat kıvrımları Euler turbo makine denklemleri yardımıyla hesaplandı.

Pompa modelleri hesaplamalı akışkanlar dinamiđi ile incelenerek her modeldeki basınç artışı ile kandaki bozulma miktarları karşılaştırıldı. Simülasyon sonuçlarında, dördüncü modelin MicroMed DeBakey modeline göre %38 oranında daha fazla basınç artışı, kandaki bozulma miktarını %6 düşürerek sağladığı görüldü.

# 1 Introduction

Cardiac failure is an important health problem which threatens human life. With the developments in technology and medical science, different treatment methods are developed. One of the most efficient treatment methods is supporting the pumping action of a failed heart via a mechanical system. This mechanical system is called blood pump. Blood pumps can be classified into two main categories as total artificial hearts and assist devices. Total artificial hearts replace a failed heart. On the other hand, assist devices support the failed heart. Assist devices have also different kinds as displacement pumps and rotary blood pumps. Axial blood pump is a rotary blood pump which provides blood flow in axial direction.

There are numerous studies on axial blood pumps in recent years. In 2007 Chua et al. investigated an axial blood pump which is based on a prototype developed in Nanyang Technological University. The simulation results showed that the pump generate a mass flow rate of 5.4 l/min and 13 332 Pa of pressure rise at 11 000 rpm. [1]

In 2006 another study was done to achieve an optimized impeller geometry by Triep et al. Three different rotor geometries were investigated via CFD and a test mechanism. The results are in an agreement with each other. Finally the optimized model could generate 2.4 l/min mass flow rate at 6666 Pa with a rotational speed at 45 000 rpm. [2]

In 2003, hemolysis in an axial blood pump was investigated by Mitoh et al. CFD and experimental results of four different impeller geometries are compared. Simulations were done at different rotational speeds. At the end of the study, most suitable geometry was determined. Simulation results showed that higher rotational speeds cause an increase in hemolysis rates. [3]

In 2006, Zhang et al. made a study to decrease the hemolysis rates in an axial blood pump. They aimed to eliminate the leakage flow by a novel integrated rotor geometry. [4]

Another study is done by Untaroiu et al. in 2005. They examined the influence of the diffuser blades in an axial blood pump. The models with different number of diffuser blades are investigated for different rotational speeds. [5]

In 2004, Song et al. aimed an idealize blood flow path. They designed four different models and then compared the simulation results. The effect of different blade geometries on blood flow is investigated. [6]

In 1996, Anai et al. investigated the relationship between rotational speed and the hemolysis. Results showed that the lower pump speeds cause decreased hemolysis. [7]

In our study it is aimed to design an axial blood pump which generates high pressure with the minimum blood damage. Thus different axial blood pumps are numerically simulated via computational fluid dynamics (CFD) and compared. All simulations were done for 6 l/min of mass flow rate at 10 000 rpm. The first investigated pump is MicroMed DeBakey LVAD which is also the baseline of this study. MicroMed DeBakey LVAD is chosen because it is a widely used axial blood pump in the clinical setting. Secondly, an optimization study model, which is generated by parametric design is investigated. Thirdly, an axial blood pump model is created by using arc-shaped blades. In this method cambers resemble an arc geometry. As a fourth design, the blades are designed by aiming constant pressure rise through the blades. The Euler turbomachinery equation is used here. The strategy is dividing the blades into ten equal sections in axial direction and generating constant pressure increase through the sections. Inlet and outlet angles are also calculated for each section.

The simulation results of each model are compared with each other. Best results are achieved with the fourth design. It provided a pressure rise of 10 856 Pa is generated for 6 l/min of mass flow rate at 10 000 rpm. In other words %38 higher pressure rise with %6 lower wall shear stress (WSS) level than the baseline design is achieved.

The thesis is divided into two main sections. At the first section, physiologic system and the design process of an axial pump is introduced theoretically. At the second section, axial blood pump models with different design methods and their simulation results are given.

## 2 Theory

### 2.1 Physiologic System

#### 2.1.1 Circulatory System

Transport of oxygen, nutrients and waste products in our body is done by the circulatory system. As briefly shown at Figure 2.1, blood leaves the heart, delivers oxygen and nutrients to the body and returns to the heart after collecting waste products of the body. Then blood flows to lungs from heart to be refreshed and return to the heart again. The system consists of blood, blood vessels and heart.

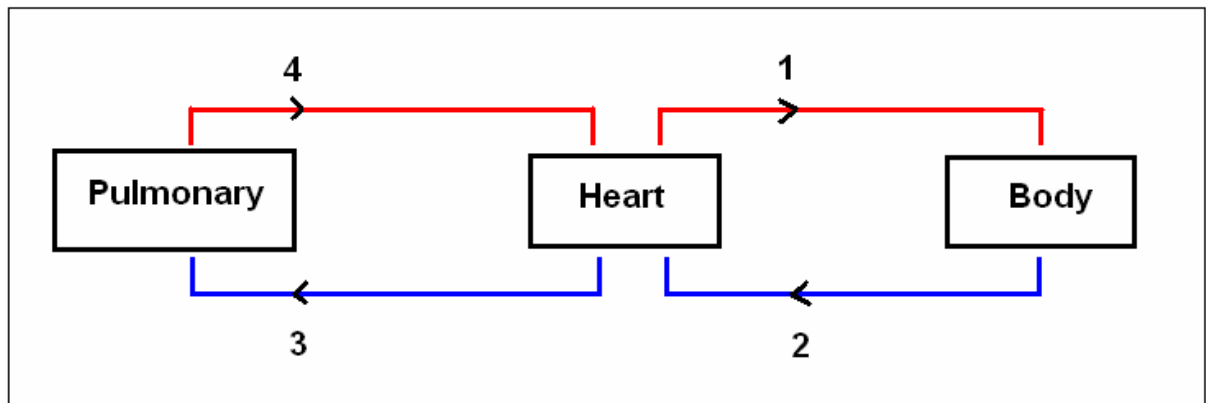


**Figure 2.1: A Basic Table of Circulation**

#### 2.1.2 Blood

During the circulation, blood transports the substances, which our body needs to have and get rid of. Blood is comprised of plasma and cells, which are platelets, red blood cells and white blood cells. Forty five percent of blood is cells and fifty five percent is plasma. Plasma is the liquid component of blood. Ninety percent of plasma is water and ten percent is dissolved minerals which are nutrients (proteins, salts, glucose), wastes (eg. urea, creatine), hormones and enzymes.

#### 2.1.3 Blood Vessels

Blood vessels are tubes which carry blood. They can be classified as arteries, veins and capillaries. Blood is carried away from the heart by arteries and returned to the heart by veins. The abdominal aorta's diameter normally ranges from 1,9 to 2,54 centimeters. [9]



Capillaries are the smallest blood vessels which are 5–10 $\mu$ m in diameter. They are connected to arteries and veins. They allow transfer of substances between blood and surrounding tissues.

#### **2.1.4 Heart**

Heart is a muscular pump which is located in the left handside of chest. It pumps blood through the blood vessels at each heartbeat. The average number of heartbeats per minute is 72 for an adult human. It means that, approximately 2.5 billion heartbeats occur throughout an average of 66 years of human life. Heart is divided into two parts: right and left side. Each side of the heart includes the atrium and the ventricle. These sides prevent mixing of oxygen rich blood and oxygen poor blood.

#### **2.1.5 Circulation**

Circulation is a two stage process. At one of these stages, oxygen rich blood is taken from lungs and pumped to the body by the left side of the heart. This is called the left circulatory system. At the other stage, oxygen poor blood is taken from the body and pumped to the lungs by the right side of heart. This is called the right circulatory system. There are four valves in the heart to keep blood moving in the correct direction. They are called as tricuspid, mitral, pulmonary and aortic valves which are opened only one way and once per heartbeat. The oxygen poor blood is taken to right ventricle from right atrium by the tricuspid and sent to the pulmonary artery from the pulmonary valve. Then the oxygen rich blood is taken to left ventricle from left atrium by the mitral valve and sent to the aorta by the aortic valve.

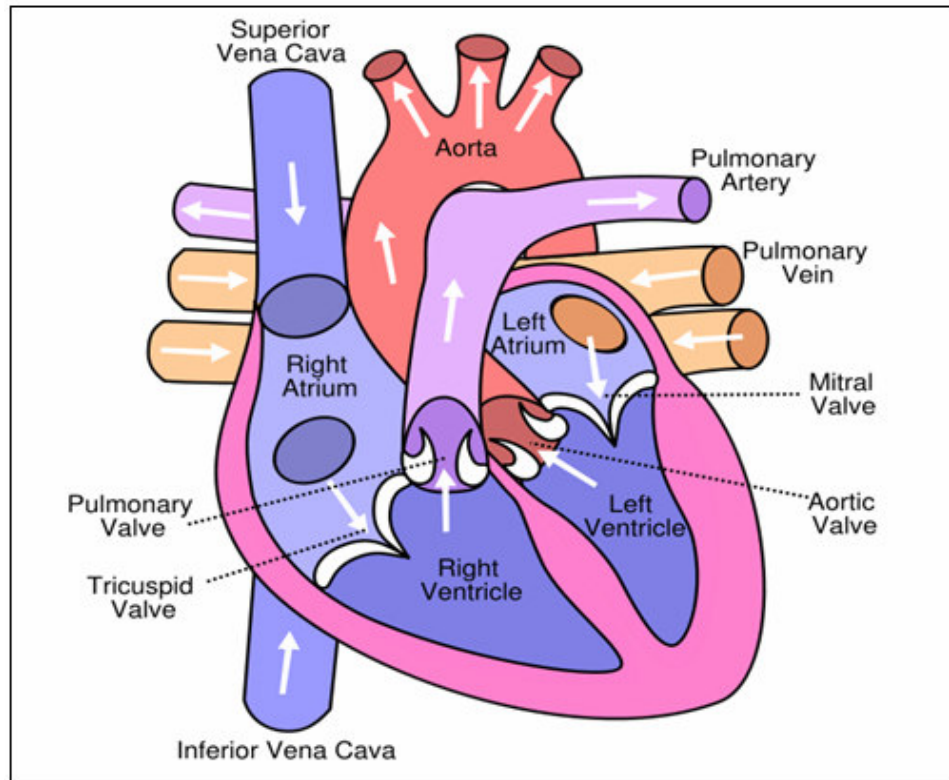


**Figure 2.2: Heart and Circulation**

### 2.1.6 Cardiac Failure

Cardiac failure is a significant and frequently seen health problem all over the world. Each year it causes millions of deaths as seen in the table below. [8]

**Table 1: Causes of death in the United States of America (2002) and Germany (2004)**

Cause of death	United States	Germany
Heart and circulatory diseases	859 619 (35%)	338 222 (45%)
Cancer	557 271 (23%)	209 477 (26%)
Respiratory diseases	124 816 (5%)	52 369 (6%)
Accidents	106 742 (4%)	33 549 (4%)
Other	721 690 (33%)	154 653 (17%)

Heart transplantation is one of the surgical therapeutic modalities in the end stage cardiac failure. This method is an effective treatment but the number of donors is not enough because there are many people waiting for transplantation. Thus many of patients

die awaiting for a heart transplantation. To overcome these limitations, scientists have started to investigate mechanical solutions to support failed heart until the transplantation.

## **2.1.7 Mechanical Solutions**

### **2.1.8 History**

The main reason of using a cardiovascular assist device is the recovery of a failing heart or as a mechanical bridge to transplantation. The idea of supporting a failed heart with a device has been proposed by LeGallois in 1812. An artificial heart was discussed and planned in 1930s by Linderbergh and Carrel. In 1953, cardiopulmonary bypass was introduced by Gibbon. It was a revolution for heart surgery and this showed a medical device could replace the function of the heart. In 1959, Spencer showed that a failed heart could be assisted by a circulatory support. The first mechanical assist device was successfully used to aid a failing heart by DeBakey in 1963. The first implantable device was used as a bridge to transplantation by Cooley in 1969. In the 1970s and 1980s, further researches were continued. In 1982, DeVries implanted a total artificial heart into a patient and the patient survived for 112 days after implantation. However due to the high thrombosis and infection risks, the use of total artificial hearts were decreased by the end of 1980s. At the same time the idea of supporting a failed heart with a device until transplantation became stronger. Today both total artificial hearts and assist devices are treatment options for cardiac heart failure. [10]

## 2.1.9 Blood Pumps

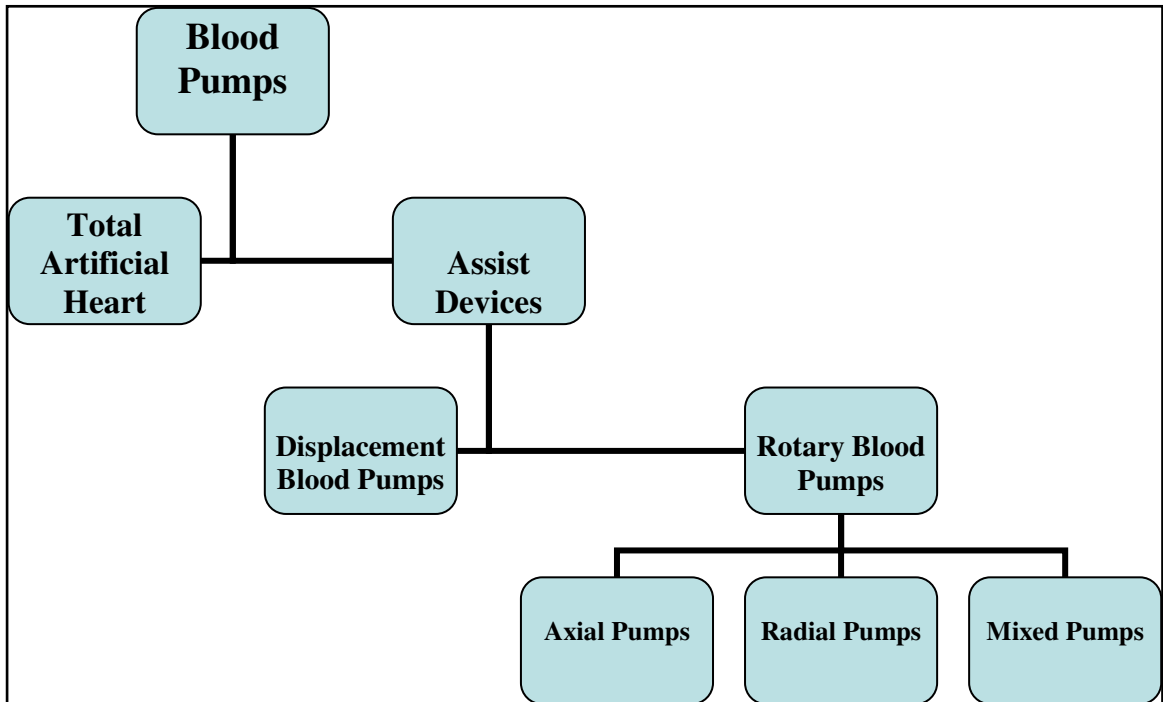


**Figure 2.3: Classification of Blood Pumps**

Mechanical circulatory support can be classified into two main categories that include total artificial hearts and assist devices. Displacement blood pumps and rotary blood pumps are both assist devices. A failed heart is supported by assist devices until the transplantation. Using an assist device often allows the heart to rest and to become stronger before the transplantation. On the other hand, a total artificial heart replaces the failing heart by anatomically and functionally. By ventricular assist devices, right ventricle or left ventricle can be supported. It is also possible to support both right and left ventricle. Left ventricular assist devices (LVAD) are most commonly used. However if resistance of pulmonary arterial is high, right ventricular assist device becomes necessary.

### 2.1.9.1 Total Artificial Heart

A total artificial heart device aims to take over the pumping job from the failed heart. The native heart is replaced with the total artificial heart device until the transplantation. Thus the device supports the body not the failed heart. In 1969, Cooley did the first implantation of a total artificial heart. Liotta designed the pump with two parts and the aim was to support the patient until the transplantation. It was a pneumatically powered device and was connected to an external power unit. The direction of blood flow was

controlled by valves. Device used in a 47 year old patient and it supported the body for 64 hours until the donors heart was transplanted. The device was not used clinically again but it was proven that a total artificial heart can be used safely as a bridge to transplantation. [10]

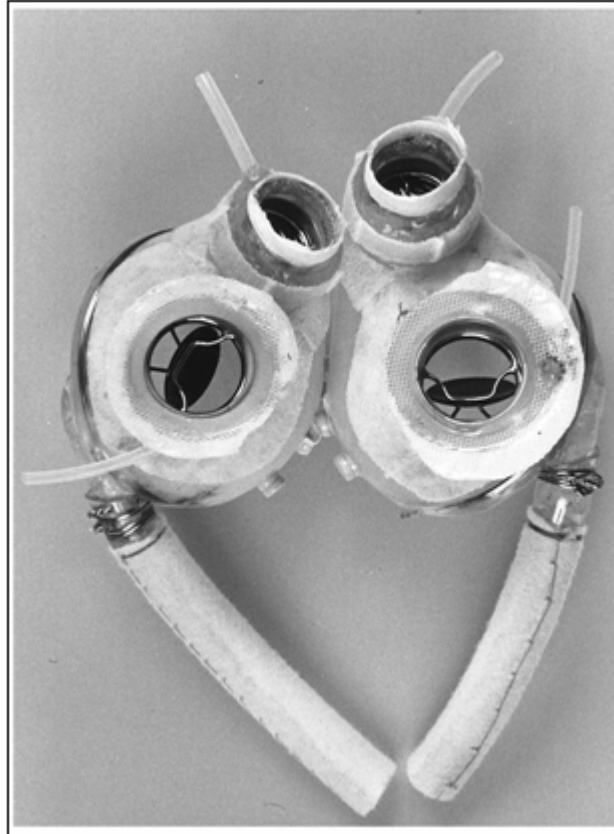


**Figure 2.4: The Liotta total artificial heart, the first one implanted in a human.**

After the first experience of the total artificial heart implantation, more models such as Akutsu-III, Jarvik-7 and Abicor have been designed and used.

### **2.1.9.2 Displacement Blood Pumps**

Displacement blood pumps are pulsatile assist devices, which pump blood like the natural pulsing action of the heart. They use mechanical force to push a fixed volume of fluid from the inlet of the pump to the outlet of the pump. The rate of power per unit weigh (power density) is high at the displacement pumps. These pumps are capable to generate high pressure rises. However displacement pumps are generally larger than equal capacity hydraulic pumps. Another disadvantage of these devices is its higher costs. The Heartmate LVAD can be given as an example to displacement blood pumps. It was designed in 1975.

It was a pneumatic vented system at first. But in 1991, the model was developed as electric vented with portable batteries. Device has an external housing which is made of titanium. Stroke volume of the device is 83 ml and the pumping capacity is 10 l/min. Device is placed into the left upper quadrant of the abdomen as shown in Figure 2.5 below. [10]

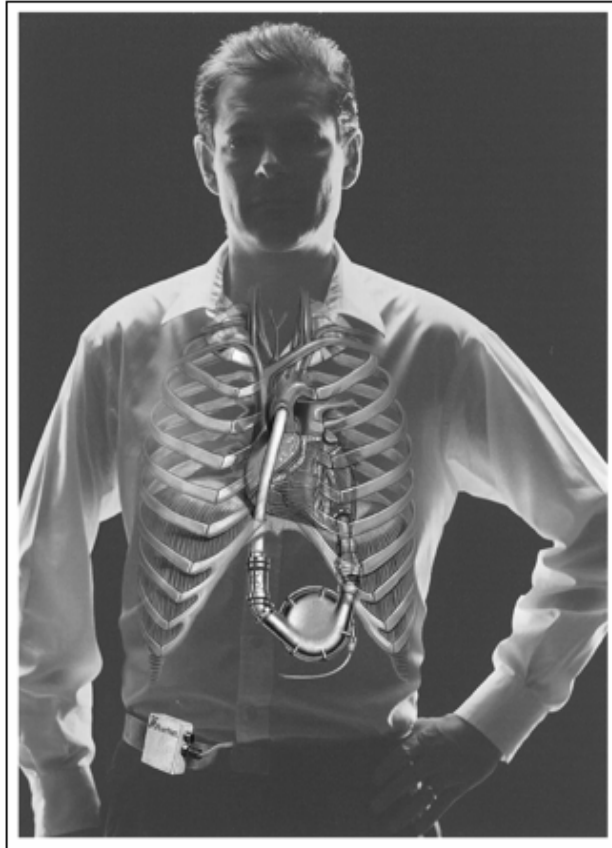


**Figure 2.5 Heartmate LVAD**

There are also different displacement pump models like Novacor and Thoratec.

### **2.1.9.3 Rotary Blood Pumps**

Rotary blood pumps are generally continuous flow devices. They can be classified into three types depending on the impeller geometry: axial, radial and diagonal. All types have a central rotor. Systems often contain permanent magnets. Battery units supply electric to coils in the pump housing and forces are applied to the magnets by the electric running through the coils. These magnetic forces make rotor to rotate.

### **2.1.9.3.1 Axial Blood Pumps**

Blood is accelerated axially by a rotating impeller with a high rotational speed. Axial pumps have some advantages as smaller sizes, less power consumption, less blood contacting surface area, minimal moving parts and no valves. On the other hand, because of its high rotor speed, axial blood pumps have a risk of blood damage. During the studies and researches between 1960s and 2000s, numerous axial pumps models have been designed. MicroMed DeBakey VAD, Heartmate II and Jarvik 2000 pump models can be given as an example to axial blood pumps. [1]

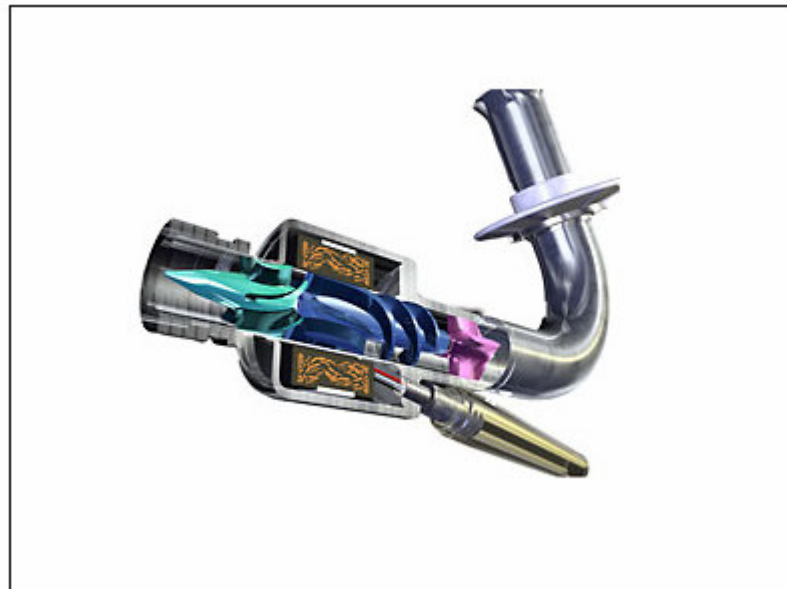


**Figure 2.6: MicroMed DeBakey ventricular assist device.**

### **2.1.9.3.2 Radial Blood Pumps**

Centrifugal pump generates pressure rise with the help of centrifugal action. It consists of three main parts which are the impeller, the volute casing and the diffuser. Centrifugal pumps work with lower specific speeds (500-1500) than mixed and axial pumps. Fluid is radially forced and accelerated at the impeller. Then fluid leaves the impeller with high velocities. The kinetic energy is transformed to pressure rise at the diffuser section, which can be both vaneless or vaned. After the diffuser, fluid moves into volute casing. Volute section provides fluid flow from diffuser to outlet of the pump. [13]

A centrifugal assist device was first used in 1989 at the Royal Children's Hospital in Melbourne, Australia. [14] After the first experience, different researches have been done and several models were designed. An example to centrifugal assist device is shown in Figure 2.7 below.

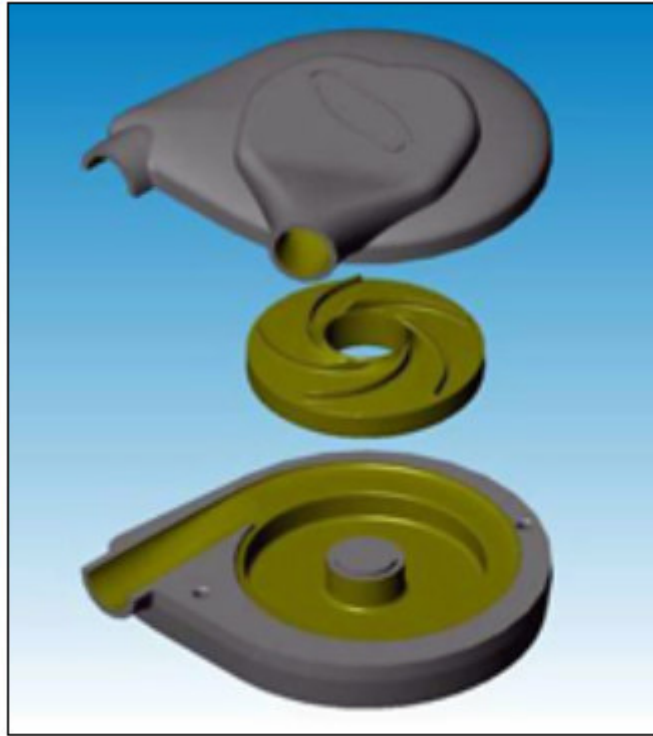


**Figure 2.7: Levacor Ventricular Assist Device**

### ***2.1.9.3.3 Mixed Blood Pumps***

The unique characteristic of mixed blood pumps is that the fluid has both axial and radial movement through the device.

Different mixed blood pump models are developed for treatment of ventricular failure. VentrAssist, HeartQuest, DeltaStream and PediPump can be given as an example to mixed flow ventricular assist devices. [12] The solid model of Pedipump assist device is shown in Figure 2.8.



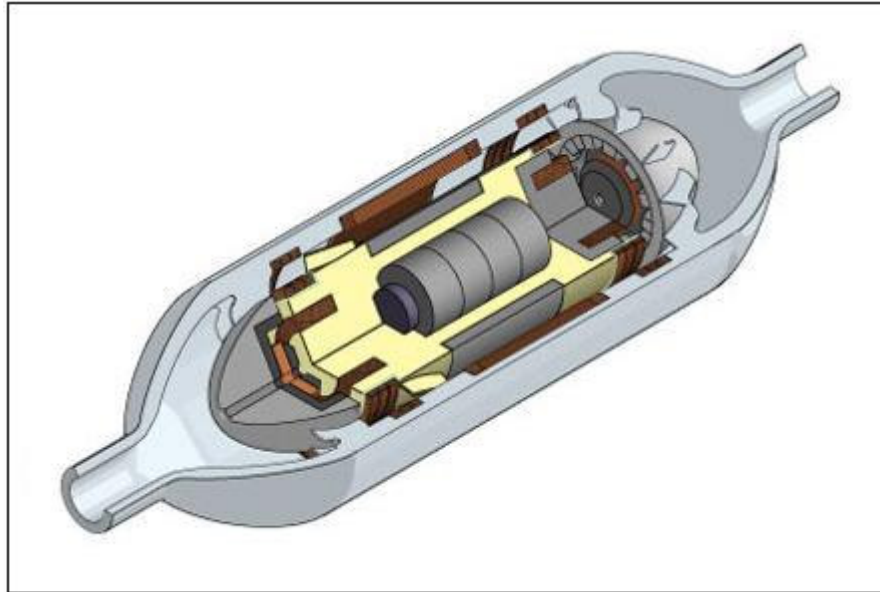


**Figure 2.8: PediPump assist device.**

### **2.1.10 Complications**

The interaction between the pump and the blood is very important. Using a blood pump as a bridge to transplantation can cause some serious complications. The most important complications are infection, postoperative bleeding, thromboembolism and hemolysis. [10]

There is always a risk of infection during the implantation. It occurs especially in critically ill patients at any phase of circulatory support. The rate of infection has been decreased in the more recent experiences.

Thromboembolism is one of the complications which is related with blood and device interface. The blood damage rate due to the thromboembolism varies from 7% to 47%. Blood pumps are generally required an anticoagulant therapy to prevent thrombosis. Cardiac failure patients often take anticoagulants also before the blood pump implantation. Thus the coagulation rate of blood decreases and postoperative bleeding risk occurs. On the other hand it is necessary to use anticoagulants against thromboembolism risk. A balance between preventing and allowing blood to clot should be provided during the anticoagulant therapy.

Postoperative bleeding occurs after the placement of device. Surgical dissection, anticoagulant therapy or human-device interaction failure can cause postoperative

bleeding. These complications occur in nearly 40% to 50% of blood pump recipients.

Hemolysis is damage of red blood cells which is a serious problem. It is caused by high shear stresses and the exposure time. [1]

Just one of these complications can lead to multiorgan failure which is the most frequently cause of death in blood pump recipients. Finally when a blood pump is being designed, the complications should be considered with hydraulic requirements.

## **2.2 Design of an Axial Blood Pump**

Important characteristics of human body, blood flow and blood should be considered when a blood pump is designed. First of all, device should pump blood with minimum hemolysis and thrombus formation. In other words it should be biocompatible. To have a minimum tissue damage, pump should have low heat generation levels. The blood pump should not cause any complications to other organs. It also should be biochemically stable with body and should provide an efficient long term circulatory support. [19] Finally there should be enough flow rate of blood which is generated by blood pump against the mean aortic pressure of about 100 mmHg.

The performance of a blood pump depends on its design. As mentioned before, rotary blood pumps provide pressure rise by a rotating impeller. A well designed blood pump provides enough pressure rise with minimum blood damage.

Impeller speed, blood flow rate and pressure head are the most important parameters in the beginning of design process.

### **2.2.1 Velocity Components in a Rotating Domain**

The three components of the velocity vector can be presented as in Figure 2.9 in a turbomachine.  $V_a$  is axial,  $V_r$  is radial and  $V_\theta$  is tangential velocity. Any change in angular speed causes angular motion and it effects the tangential velocity, which is a very important parameter for design process. Magnitude of tangential velocity depends on impellers rotational speed and radius.

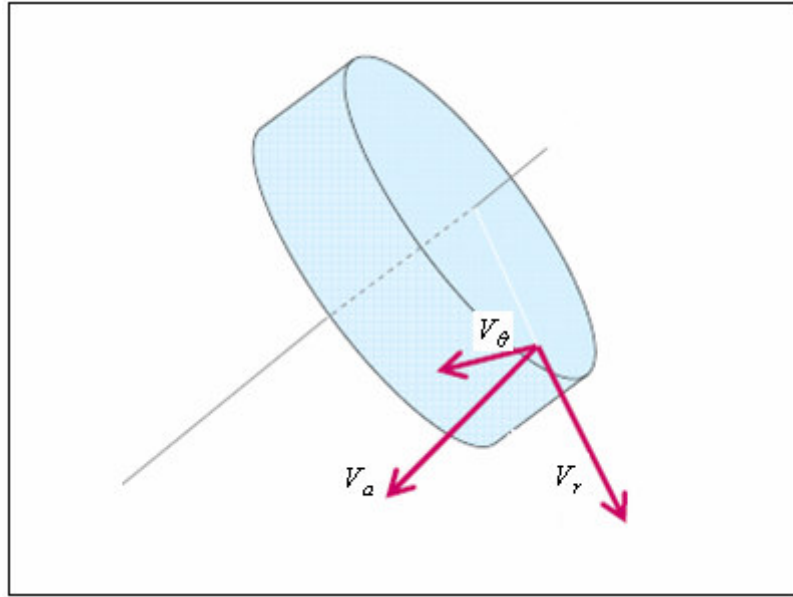


**Figure 2.9: Velocities at any point of the pump**

### 2.2.2 The Euler Turbomachinery Equation

The Euler turbomachinery equation is the basic equation of turbomachinery, which describes the work generation/consumption in terms of flow velocities. It can be applied to turbines, pumps or compressors. In the following the derivation of this equation will be given. In a rotating system torque developed can be calculated from the rate of change of angular momentum with the help of Newton's 2nd law. [16]

$$\tau = \Delta(m \cdot r \cdot V_{\theta}) = m \cdot (r_1 \cdot V_{\theta 1} - r_2 \cdot V_{\theta 2}) \quad (2.1)$$

In a steady flow process, mass flow rate remains constant. Energy which is transferred per unit mass flow rate can be calculated in terms of torque and angular velocity as follows.

$$W_x = (\tau \cdot w / m) = w \cdot (r_1 \cdot V_{\theta 1} - r_2 \cdot V_{\theta 2}) \quad (2.2)$$

$r \cdot w$  is the magnitude of blade speed, which is shown as " $U$ ". Blade speed is constant for an axial pump because of the constant blade radius.

For the steady flow in a turbomachine the First Law of Thermodynamics states that the energy transfer per unit mass flow rate is equal to the change in total enthalpy of an adiabatic process ( $\Delta H = W_x$ ). Hence, the Euler turbomachinery equation is:

$$\Delta H = H_1 - H_2 = w \cdot r \cdot (V_{\theta 1} - V_{\theta 2}) = U \cdot (V_{\theta 1} - V_{\theta 2}) \quad (2.3)$$

### 2.2.3 Velocity Triangle

Fluid velocity vectors can be classified into two main categories as relative velocity and absolute velocity. Relative velocity is denoted by  $W$  and measured with respect to the rotating system. Similarly, absolute velocity is denoted by  $C$  and measured with respect to the stationary system. Vectoral relation between blade speed, relative velocity and absolute velocity is:

$$\vec{C} = \vec{U} + \vec{W} \quad (2.4)$$

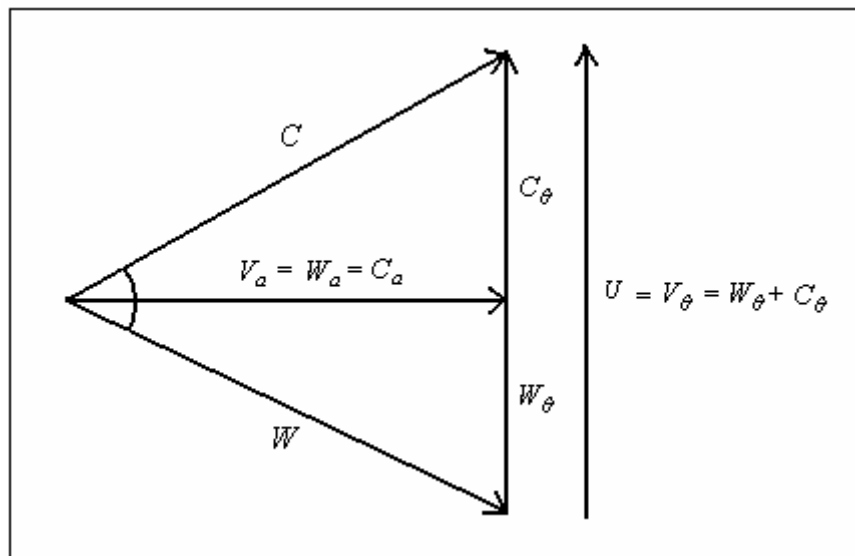


**Figure 2.10: Velocity vectors of flow**

As mentioned before,  $V_\theta$  is tangential velocity. It changes with the rotational speed and radius of the impeller. Total tangential velocity is always constant through an axial impeller and equals to the blade speed " $U$ ". In another words, sum of relative tangential velocity ( $W_\theta$ ) and absolute tangential velocity ( $C_\theta$ ) is always constant.

$$V_\theta = U = \frac{2 \cdot \pi \cdot r \cdot N}{60} = W_\theta + C_\theta \quad (2.5)$$

$N$  is number of revolutions per minute which is done by impeller.

The second important velocity is blood flow velocity in axial direction. It is denoted by “ $V_a$ ”.  $V_a$  is always constant for steady and incompressible flow. It is also the axial component of both relative and absolute velocities.

$$V_a = \frac{\rho \cdot A}{\dot{m}} = W_a = C_a \quad (2.6)$$

$A$  is area ( $m^2$ ),  $\rho$  is the density of blood ( $kg/m^3$ ) and  $\dot{m}$  is mass flow rate ( $kg/s$ ).

## 3 Design and CFD

### 3.1 Introduction

Different axial blood pump models are designed, investigated and compared in this study. The first axial blood pump, which is investigated is MicroMed DeBakey LVAD. MicroMed DeBakey LVAD is chosen because it is one of the most preferred axial blood pumps in the clinical setting.

At the second step an optimization study model was investigated, which was generated by the parametric design. The MicroMed DeBakey LVAD was selected as the baseline model. The other models were generated by using eleven parameters. However as the number of parameters is limited, there are always some geometrical limitations. [17]

The third model is generated by using arc-shaped blades. The Euler turbomachinery equation is used to calculate the inlet and outlet angles of blades. Then an arc is generated by using the following parameters: inlet angle, outlet angle and the length in axial direction of blades.

The last design is generated by aiming a constant pressure increase through the blades. Euler turbomachinery equations are used to perform the calculations. The blades are divided into ten equal parts in axial direction and the inlet and outlet angles were calculated for each section. Later, some modifications are done in section lengths of axial direction and new models are created, in order to improve the blade shape, simulation results of modified models are compared and the one which gives the best performance is chosen.

Finally the four axial blood pumps, which are introduced above are compared.

There are some common and important characteristics of axial blood pump models. In an axial blood pump, the aim is taking blood from left ventricle and pump to the aorta with enough pressure rise and minimum blood damage.

Increase in static pressure of blood is expected through the assist device. This is provided by the energy transformations. First of all, the kinetic energy which is generated by the rotational speed in impeller is transferred to the enthalpy of the fluid. Since blood is incompressible, a pressure rise is generated. Axial flow speed is always constant through the pump. The kinetic energy rise is supplied by the rotational speed and the changes in tangential flow velocity.

Device has three main parts called as inducer, impeller and diffuser. Blood leaves the left ventricle and enters to the pump. Inducer is the first stationary part of the system and blood meets with inducer at first. It has four blades which are located symmetrically to each other. A straightened blood flow is aimed by using inducer before the entrance of the impeller which is rotating with 10 000 rpm.

Blood enters to the impeller after the inducer. Kinetic energy of blood is increased by the rotational speed of impeller blades. In another words, tangential component of relative velocity is increased. The aim is to transform this kinetic energy into enthalpy through the impeller blades. Due to the rotational movement, relative velocity components are used in calculations. The energy transformation from kinetic energy to enthalpy is provided by reducing relative tangential velocity through the blades.

The third part of the system is called as diffuser which is a stationary part and thus the absolute velocities are used in the calculations. As mentioned before, magnitude of total tangential velocity is always constant through the impeller. At the impeller, relative tangential velocity is decreased but absolute tangential velocity is increased at the same time. Thus the absolute tangential velocity is maximum at the inlet of diffuser. This means blood flows into diffuser with a certain kinetic energy. The aim is to transform this kinetic energy into enthalpy one more time. Just like the impeller, tangential velocity is decreased through the diffuser blades and a straightened blood flow is desired at the outlet of diffuser. Blood leaves the device and gets into the aorta after the diffuser. Changes in tangential velocities through the impeller and diffuser blades are shown in figure below.

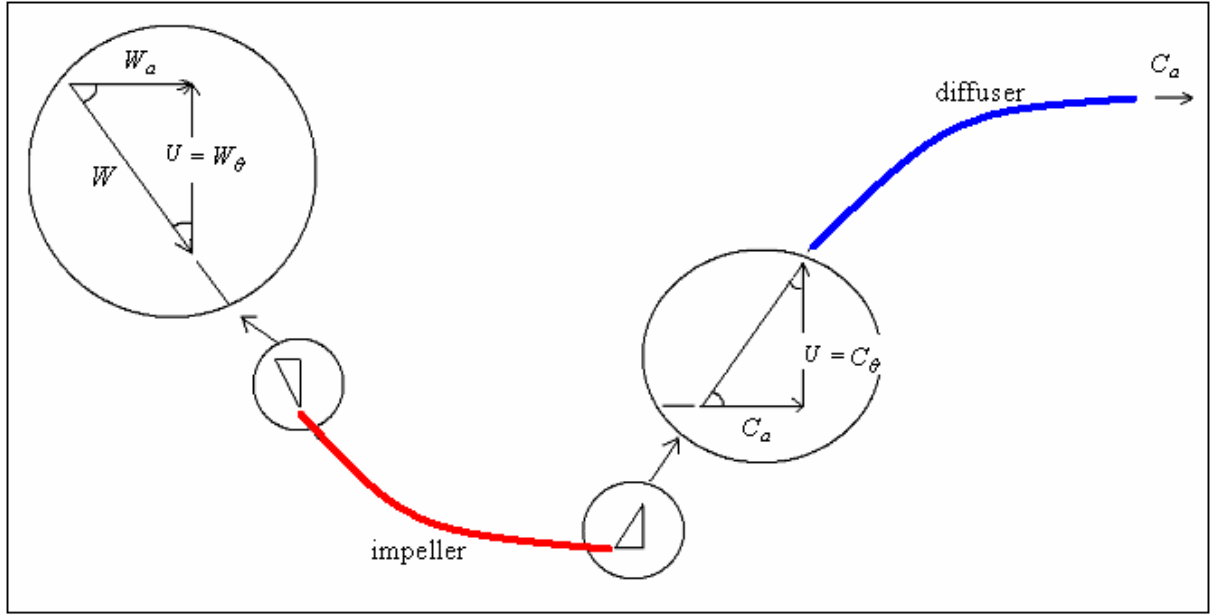


**Figure 3.1: Velocity changes through the impeller and diffuser.**

The blood flow in different axial blood pump models are investigated via CFD. The calculations were done for 10 000 rpm rotational speed and 6 lt/min mass flow rate. In all cases, computational mesh was generated by Gambit and the models were simulated by Fluent. Tetrahedral meshes are used in mesh generation.

The flow domains of different axial pumps were meshed with the same mesh densities in the simulations (approximately with 300 000 elements). Thus the models were compared more accurately between each other. In our study coarse meshes were used because simulation time increases with finer meshes and there are numerous simulations were done in this study. After the models are compared and the best one is found via coarse mesh, a finer mesh can be applied to the best pump model to have more certain results.

Reynold number is calculated for 10 000 rpm as 22600 which shows that the flow through the pump is turbulent. Magnitude of free stream velocity “ $u$ ” should be known to calculate the Reynolds number.

$$u = \frac{2 \cdot \pi \cdot r_{shroud} \cdot N}{60}$$

$$u = 6.28(m/s)$$

(  $r_{shroud}$  is equal to  $0.006m$  .)

$$Re = \frac{\rho \cdot u \cdot d}{\nu} \quad (3.1)$$

$$Re = 22619$$

$\nu$  is dynamic viscosity of blood and equals to  $0.0035(kg/ms)$  .  $d$  is the diameter of shroud which is equal to  $0.012m$  .

The flow is assumed as steady at the operation point. Flow simulations are performed with k- $\epsilon$  turbulence model. It is a two equation model, which includes two extra equations to represents the turbulent properties of flow. The first variable is turbulent kinetic energy “k”. The second variable is the turbulent dissipation “ $\epsilon$ ”. In many studies k- $\epsilon$  turbulence model is used to investigate the turbulent flow of blood through a blood pump. In 2000, Anderson et al., in 2007, Chua et al., In 2006, Triep et al. used k-  $\epsilon$  turbulence model in their simulations. On the other hand some different turbulence models are also used. In 2006, Zhang et al. used S-A (Spalart Allmaras) turbulence model at the simulations. [4]

Blood is assumed to be an incompressible Newtonian fluid with constant density and viscosity. Blood has non-Newtonian properties at low shear rates. While shear rate is above  $100s^{-1}$  blood exhibits as Newtonian fluid.

The computational domain consists of a rotating zone and two stationary zones. The rotating zone surrounds the impeller. The inducer and the diffuser are surrounded by the stationary zones. Moving reference frame algorithm is used to simulate the rotation of the impeller. Stationary and rotationary zones are coupled via sliding interfaces.





**Figure 3.2: Computational Mesh**

Computational domain is extended for a distance of  $7d$  towards the inlet and outlet. (“ $d$ ” is the diameter of the shroud.) It is aimed to investigate the effect of inducer on blood flow and the flow characteristics after the diffuser by extending the computational domain.

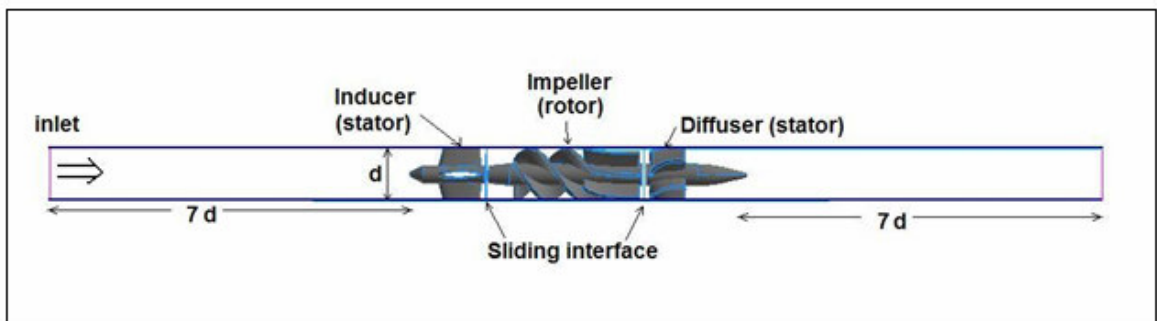


**Figure 3.3: Computational Domain**

Same boundary conditions are applied in all simulations. The boundary conditions are a mass flow inlet of  $0.105 \text{ kg/s}$  and a constant outlet pressure of  $0 \text{ Pa}$ . Turbulence intensity at the inlet is set to  $5\%$ , and the hydraulic diameter is set to  $0.012 \text{ m}$ , which is the diameter of the shroud.

To provide a more accurate simulation, the convergence criteria was chosen  $0.0001$ . [1] When the criteria is chosen  $0.00001$ , the simulation results are not changed dramatically. The change of pressure rise between these two convergence is about  $\%0.06$  and the WSS difference is about  $\%0.003$ . Thus the results are acceptable for the convergence criteria of  $0.0001$ . Also to converge the same simulation with a convergence criteria of  $0.00001$  takes a longer time of approximately 45 minutes.

To achieve a high grid quality, meshes were generated with different densities. Especially the critical flow regions like blade tip and blade inlet and outlet regions have a fine mesh.

### 3.2 Micromed DeBakey LVAD

The Micromed DeBakey LVAD is a micro axial pump, which provides blood flow from left ventricle to aorta. The device was developed by Dr. George Noon and DeBakey in 1980s. The pump dimensions are 30.5 mm in diameter and 76.2 mm long. It weighs 95 grams and is made of titanium casing with an impeller and inducer. The other parts of the pump are titanium inflow cannula, a flow meter, an outflow graft and a percutaneous cable connected to battery console. Pump is capable of pumping 10 L/min but the average pump flow is 3.9 to 5.4 l/min. DeBakey has also some characteristics as less bleeding, less infection risk, less dissection during dislocating and due to its smaller size, being implantable for the patients who has small body mass index. [10] Solid model of the device is seen shown in Figure 3.4.

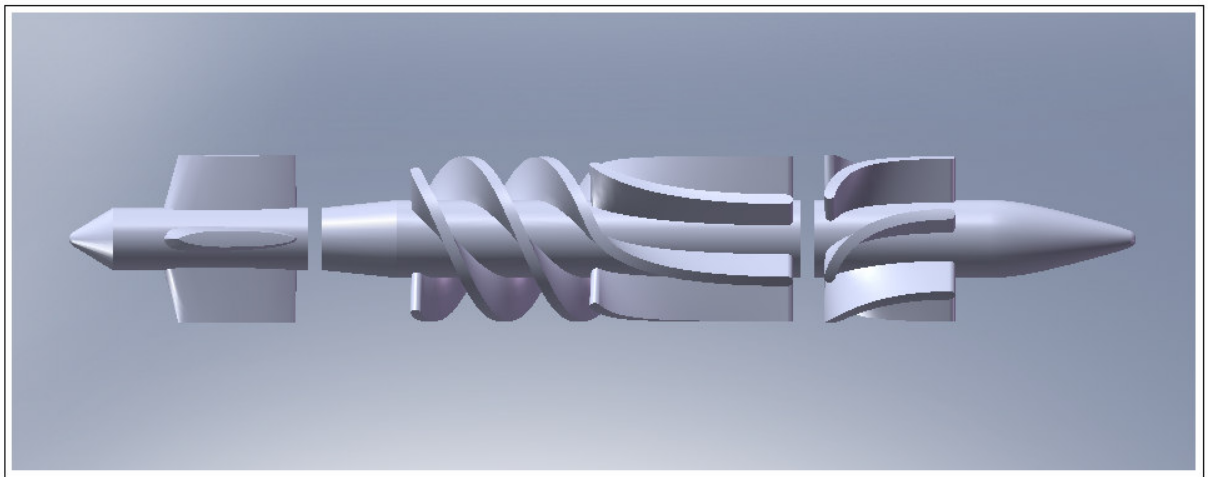


**Figure 3.4: Micromed DeBakey's solid model**

There is a flow straightener called inducer in front of the impeller. It has 4 stationary blades. Inlet angle of the impeller is  $15^\circ$  and the outlet angle of impeller is  $90^\circ$ . Impeller of device has 3 blades and there is also 3 splitters. Both splitter and impeller blades have the same tip radius value of 2.85 mm. A uniform blood flow distribution is aimed by using the splitters. Diffuser is the next and the last part of device after the impeller. Diffuser has 6

blades which are stationary and blades have an inlet angle of  $65^\circ$  and an outlet angle of  $90^\circ$ . The axial length of diffuser blades are measured 8.32 mm.

CFD simulation of the model performed with using same boundary conditions and properties which are used also at previous simulations.

### 3.2.1 Simulation Results of the MicroMed DeBakey LVAD

Pressure distribution of device is shown in Figure 3.5. The average pressure difference between inlet and outlet regions is 7 859 Pa.

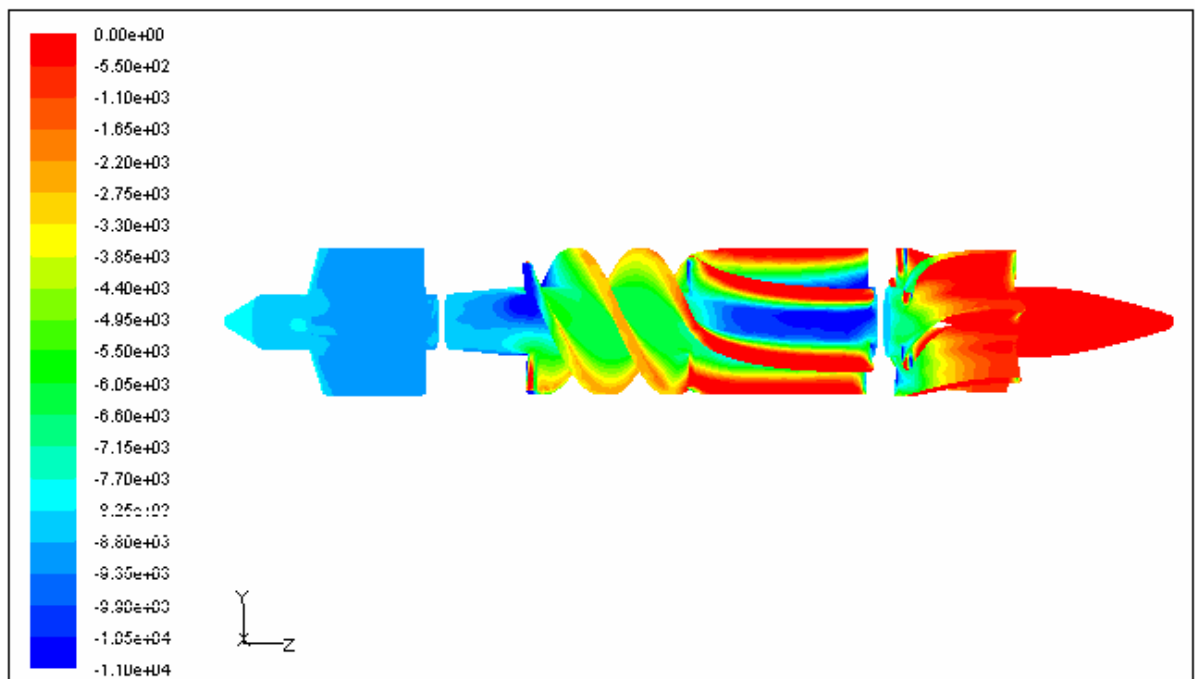


**Figure 3.5: Pressure distribution of DeBakey model**

The average WSS value at the impeller is 120 Pa.

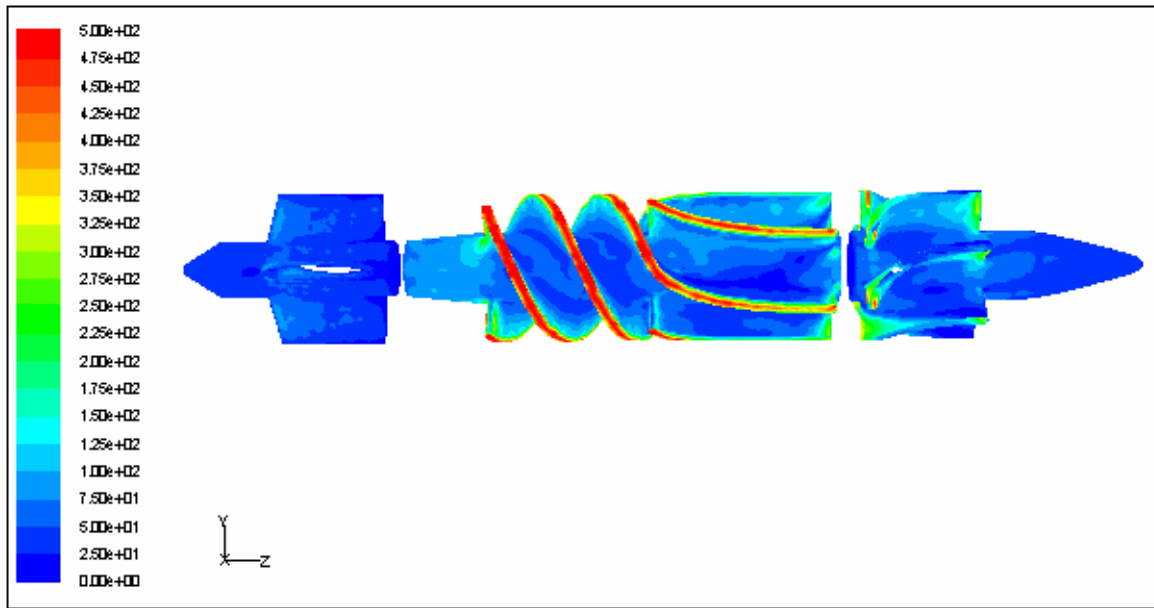


**Figure 3.6: WSS distribution of DeBakey model**

Relative velocity vectors at the impeller is shown in figure below. However splitters provide a fine distributed blood flow at the outlet region of impeller, the solid body of splitter blades cause some losses especially at the inlet of splitter blades.

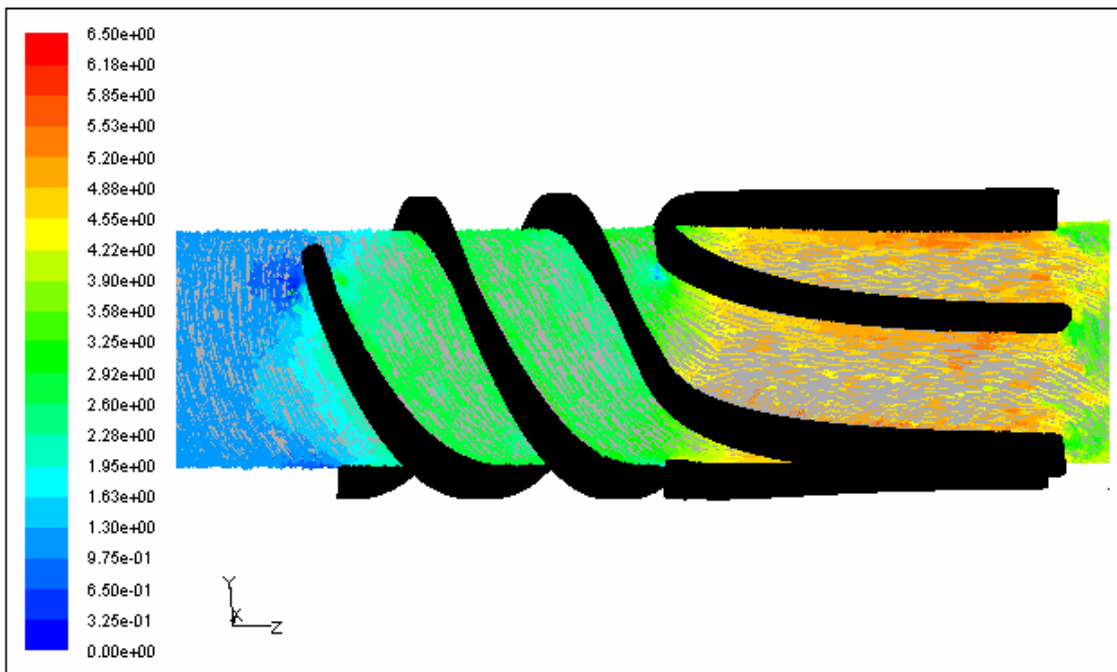


**Figure 3.7: Relative velocity vectors of the DeBakey model**

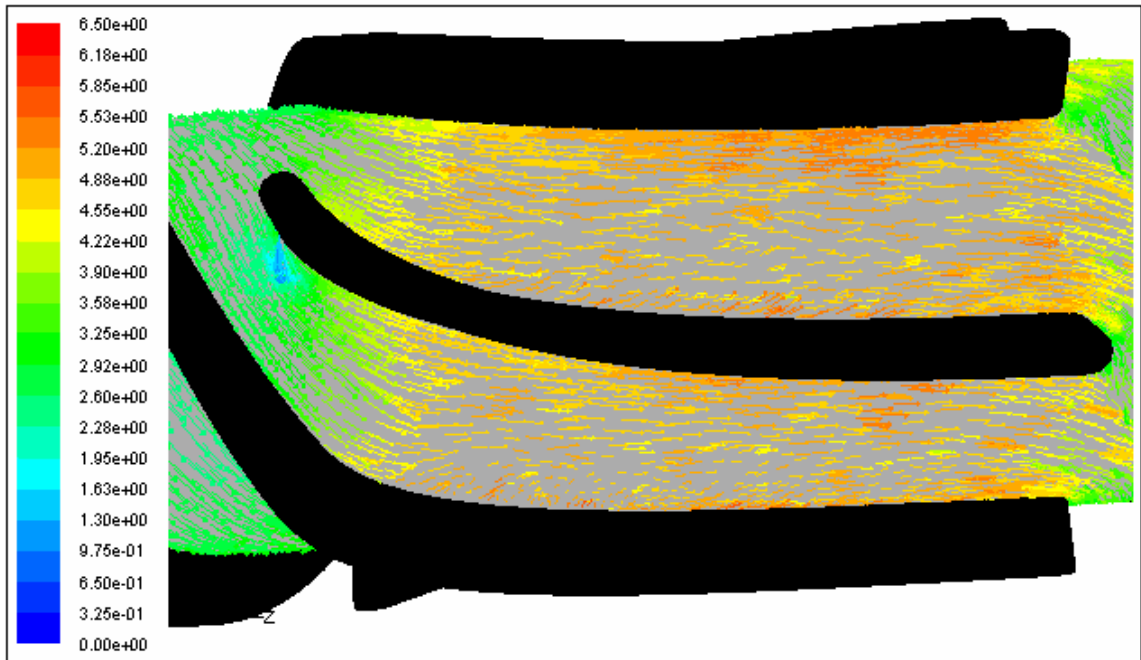


**Figure 3.8: Relative velocity vectors around the splitter blades of DeBakey model.**

Velocity vector distribution at the diffuser is shown in Figure 3.9. No flow separation occurs at the inlet. Blade inlet angle and blood flow direction is similar. However, reverse flows are visible through the blade. Also a helical flow occurs at the outlet of diffuser blade.

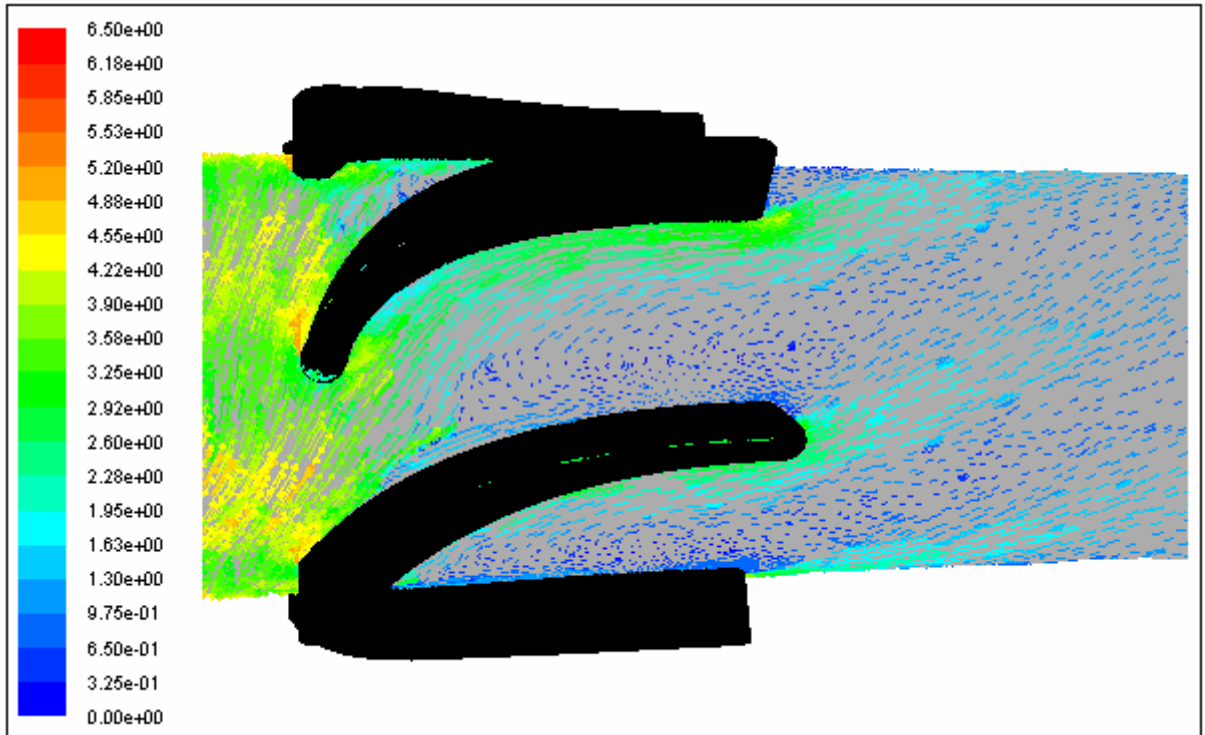


**Figure 3.9: Absolute velocity vectors around the diffuser.**

### **3.3 Optimization**

In this optimization study, it is aimed to obtain an axial blood pump geometry which provides the desired hydraulic performance with the minimum blood damage. [17] MicroMed DeBakey LVAD is chosen as a baseline and the baseline geometry is generated via parametric modeling. By using the design of experiments method, an optimization surface around the baseline design is formed. 16 different CAD models are generated based on the parametric design and these models are simulated via CFD. Then the results are evaluated and 64 more CAD models are generated. [18] Finally one of these models gave the best results. Higher pressure rise and lower blood damage rates are obtained.

#### **3.3.1 Simulation Results of the Optimization**

Pressure distribution of the optimization model is shown in Figure 3.10. 8 573 Pa of pressure rise is generated.

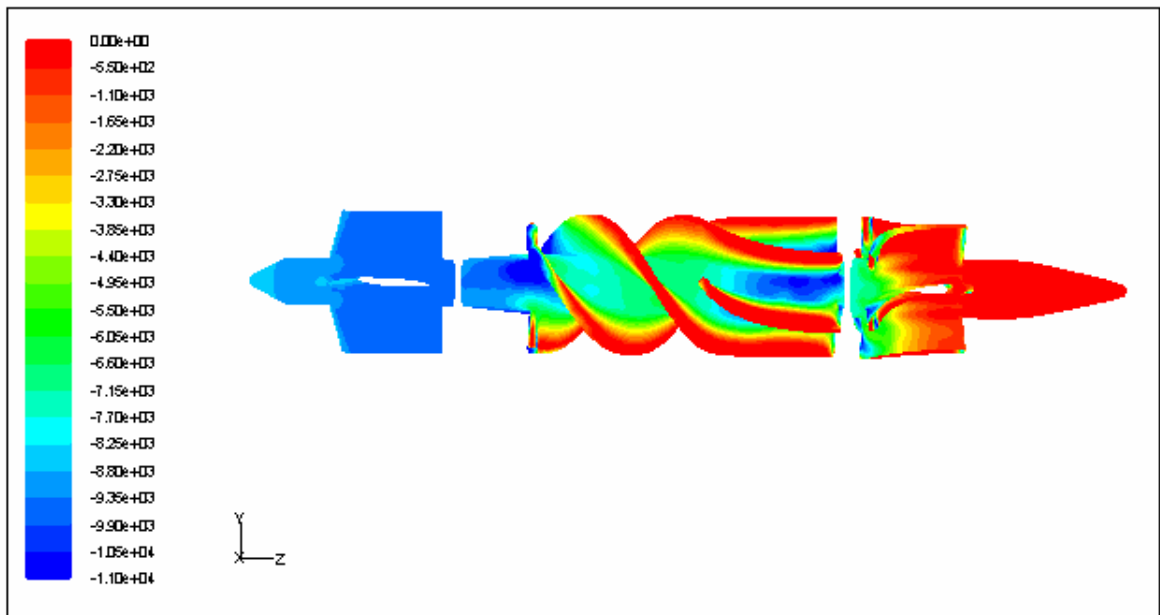


**Figure 3.10: Pressure Distribution of the Optimum**

The average WSS value at the impeller is 103 Pa.

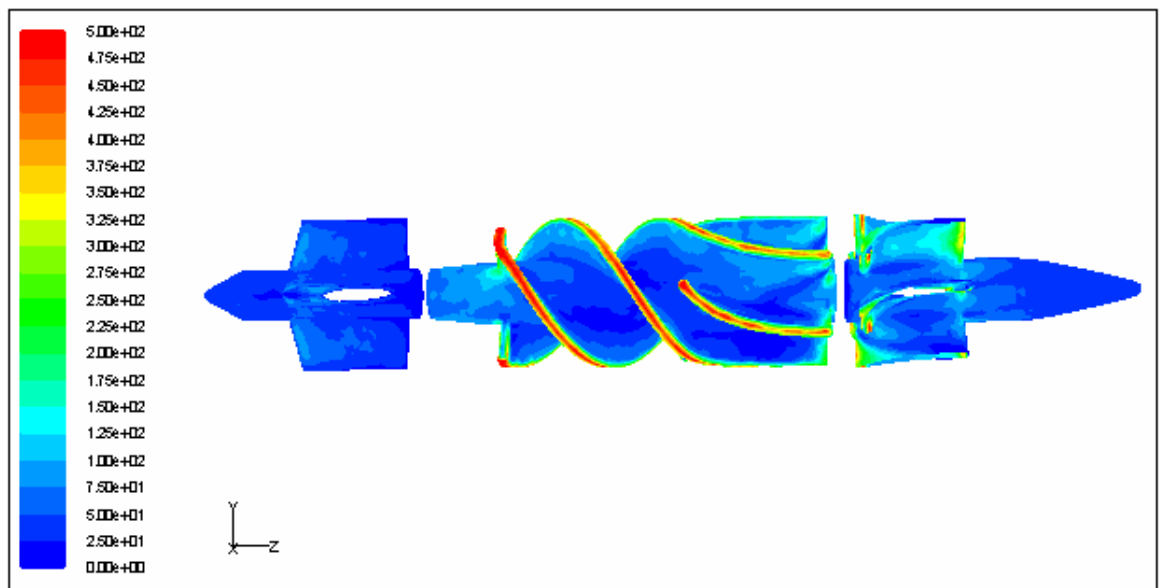


**Figure 3.11: WSS Distribution of the Optimum**

Relative velocity vectors at the impeller of optimum is shown in Figure 3.12. There are splitters also which are used at the impeller. Blade inlet angle and the flow is not similar. Thus some losses occur at the leading edge of the impeller.

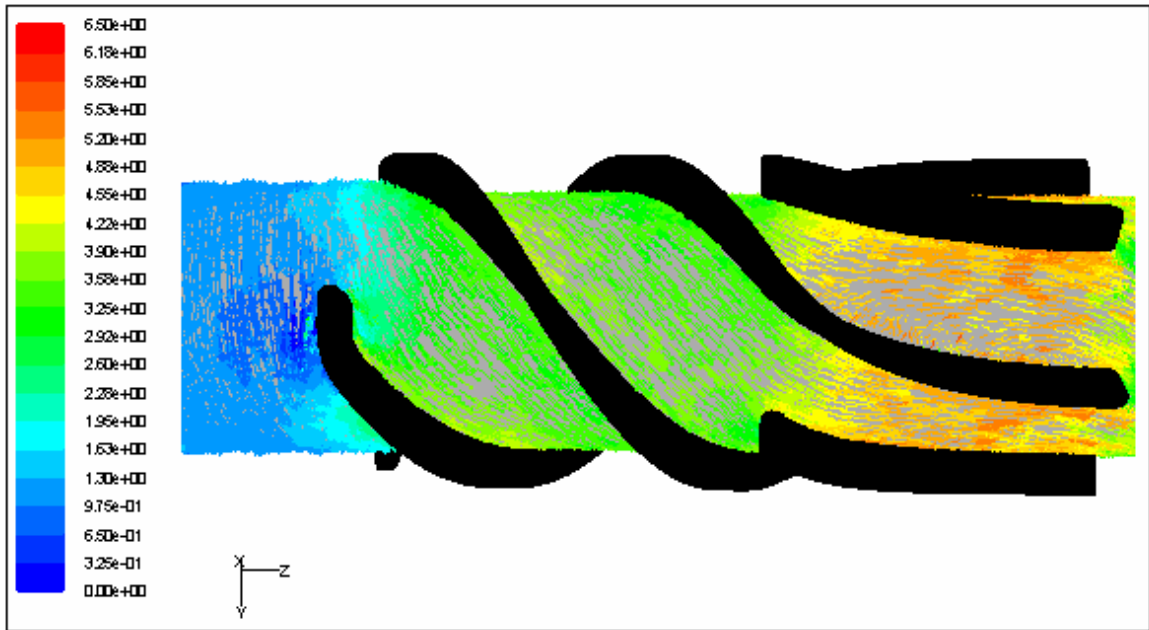


**Figure 3.12: Relative Velocity Vectors of the Optimum**

Velocity vectors at the diffuser is shown in Figure 3.13. Flow is uniform at the inlet of diffuser. There is no flow separation at the leading edge. However reverse flows and vortex formation occurs through the blades. Also the flow at the outlet of the diffuser is helical.

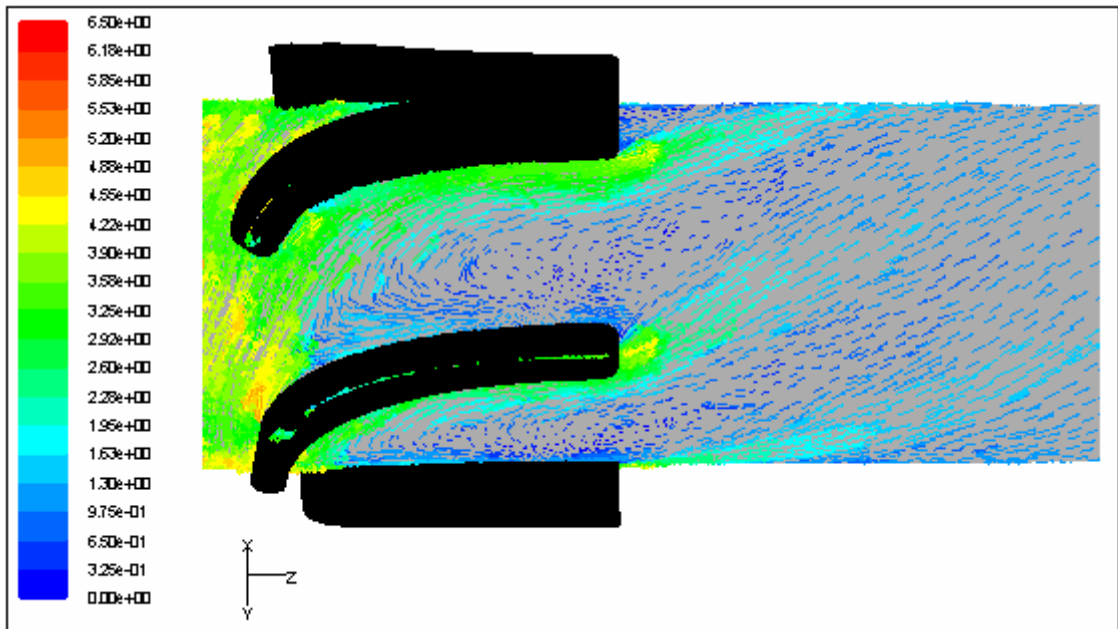


**Figure 3.13: Absolute Velocity Vectors of the Optimum**



### 3.4 Axial Pump With Arc-Shaped Blades

#### 3.4.1 Impeller Geometry

Another way of designing a blade geometry is using arcs. After the inlet and outlet angles of the impeller are calculated by using the Euler turbomachinery equation, an arc is created and wrapped around the hub. This method generally gives acceptable results at short blade designs.

Inlet angle, outlet angle and blade length in axial direction are the required parameters. The inlet angle is calculated by using the flow velocities in tangential and axial direction. The calculations are explained more comprehensively in the next section. As shown in Figure 3.14 the arc was created by using the parameters below.

Inlet angle = 25.71 deg

Outlet angle = 90 deg

Blade length in axial direction = 27.34 mm

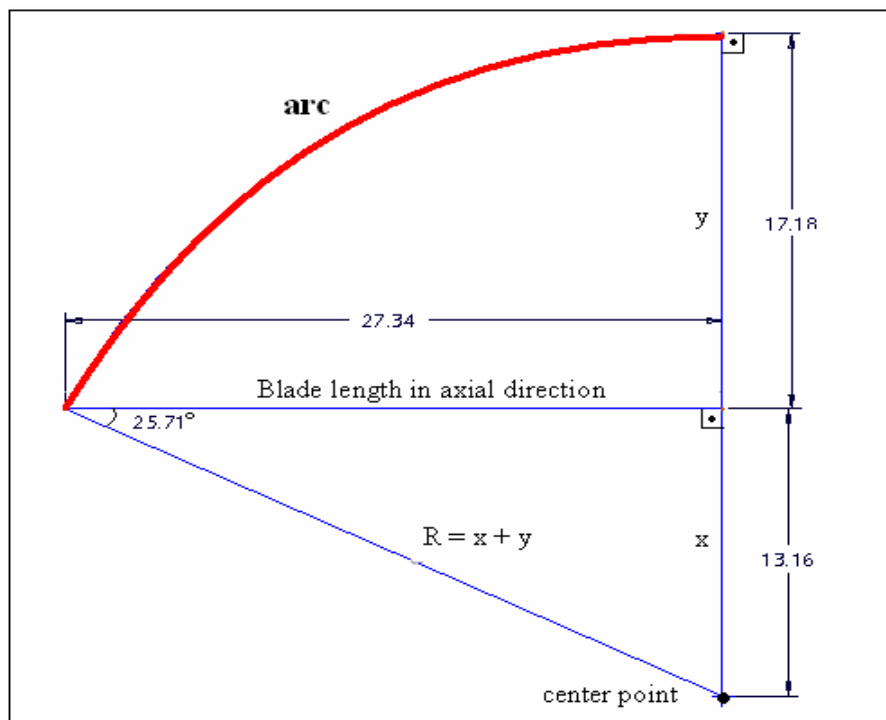
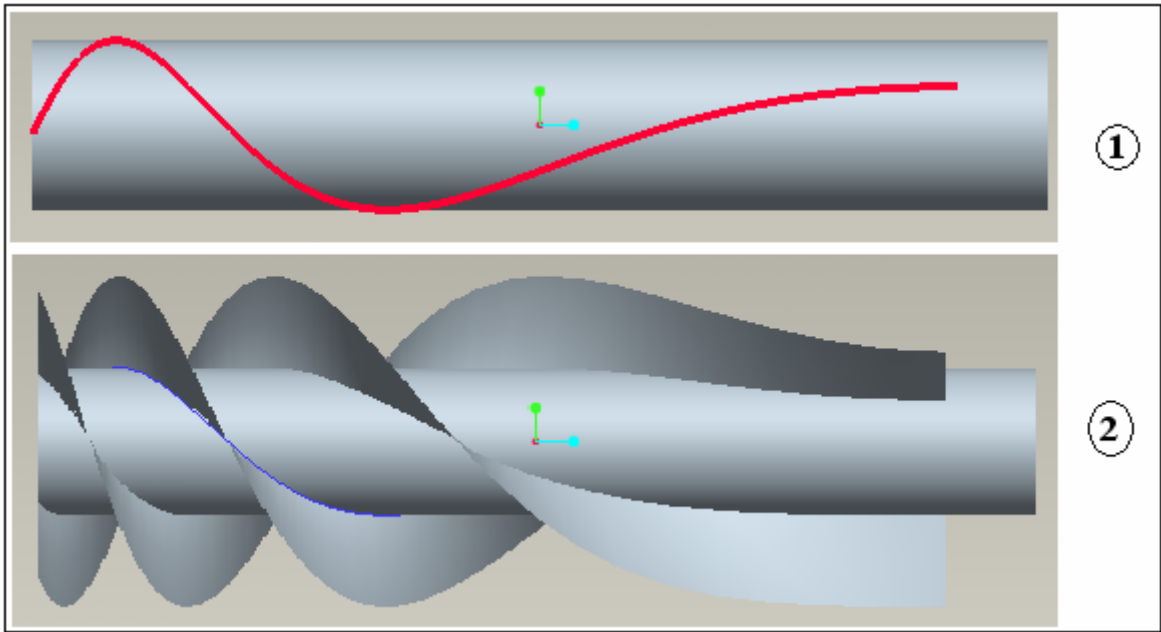
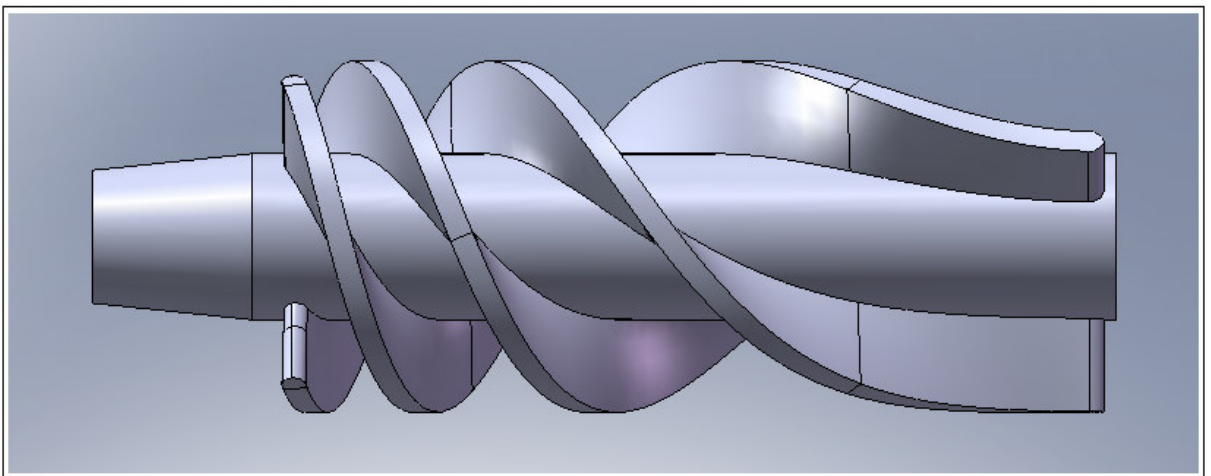


Figure 3.14: Arc creation



**Figure 3.15: Wrap around the cylinder and blade creation by arc**

After the blade geometry is created some modifications are done on the model by using solid works as seen in Figure 3.16.



**Figure 3.16: Impeller geometry designed by arc**

### 3.4.2 Diffuser Geometry

The same design method which is used for impeller is applied to the design of diffuser also. An arc is created by using inlet angle, outlet angle and the blade length in axial direction. Inlet and outlet angles of diffuser blade is the same with the impeller blades

due to the same tangential velocity magnitudes. The only difference in parameters is the length of diffuser in axial direction, which is chosen as 12.48 mm.

Inlet angle =  $25.71^\circ$

Outlet angle =  $90^\circ$

Blade length in axial direction = 12.48 mm

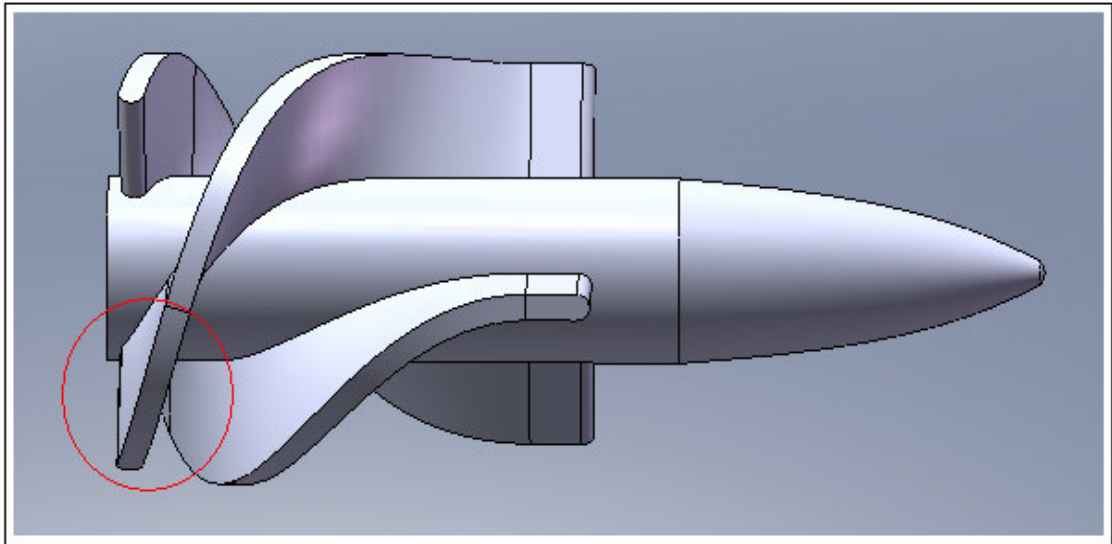


**Figure 3.17 : Diffuser geometry which is designed by using arc**

As seen in the figure above, at the inlet region of the blade the inlet angle remains constant for a distance. As a trial, the diffuser blade length is shortened for 2 mm in axial direction. The modified diffuser model is shown in Figure 3.18. Two simulations were done with the same impeller to compare diffuser models. The modified diffuser model gave better results. The pressure rise of modified diffuser model is 800 Pa more than the original one.

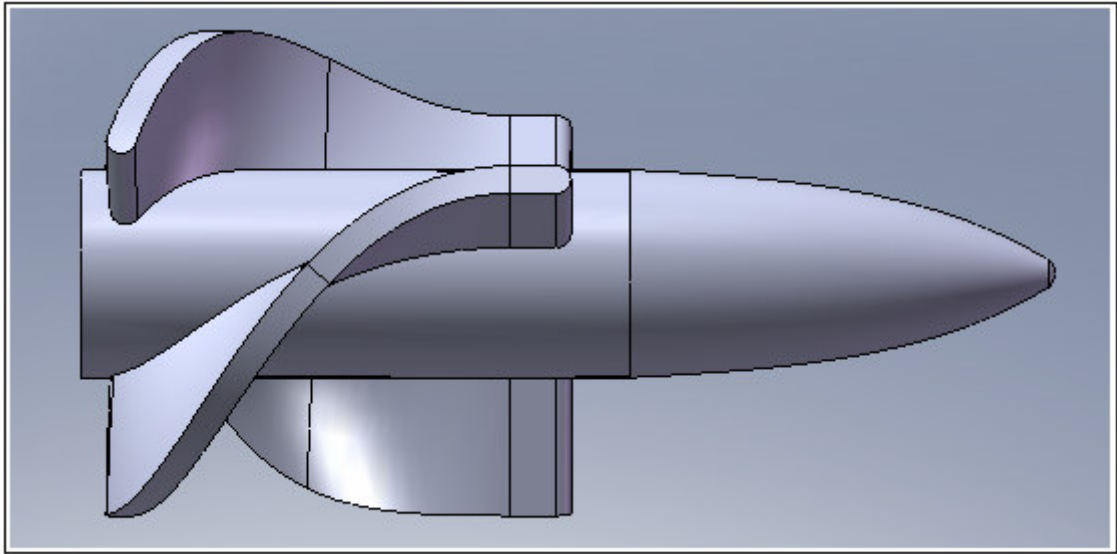


**Figure 3.18: Modified diffuser geometry which is designed by using arc.**

The whole pump model is seen in Figure 3.19. There are 0.5 mm spaces between inducer, impeller and diffuser due to the rotational movement of impeller.

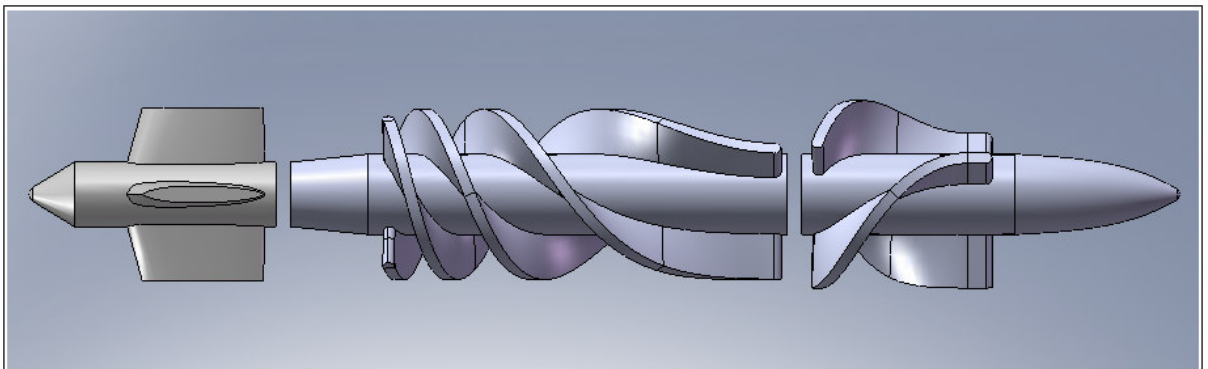


**Figure 3.19: Pump model designed by arc**

### **3.4.3 Simulation Results of Arc Geometry**

A pressure rise of 10 743 Pa was generated by the arc model.

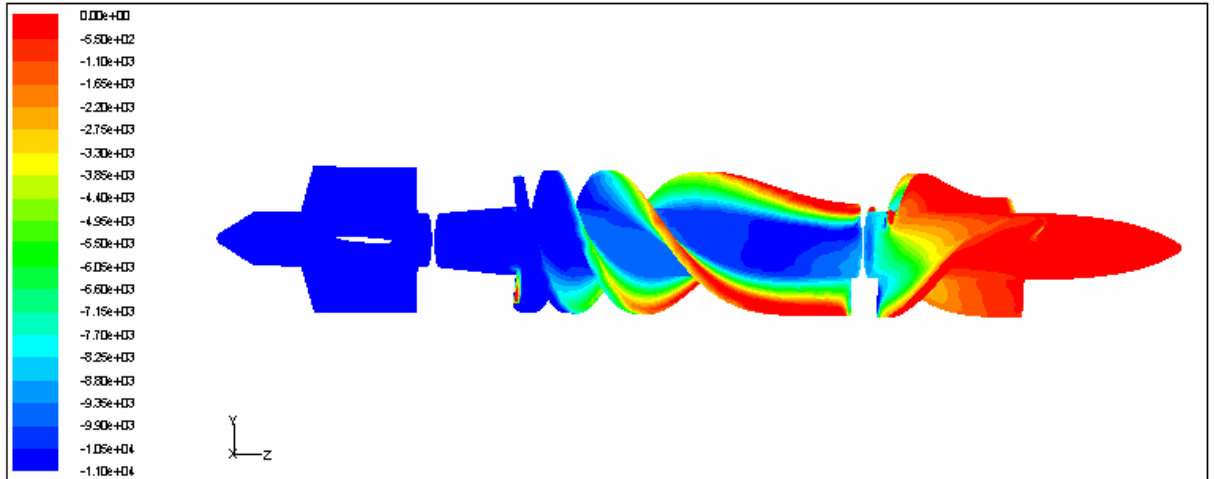


**Figure 3.20: Pressure distribution of the arc model**

The average WSS at impeller is 120 Pa.

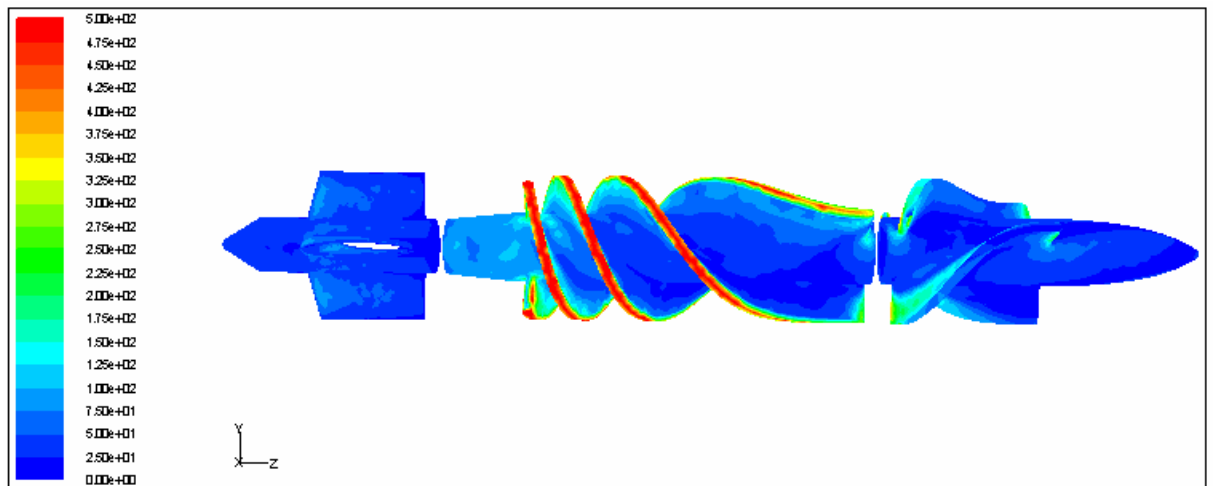


**Figure 3.21: WSS distribution of the arc model**

Distribution of the relative velocity vectors on the midplane around the impeller is shown in Figure 3.22. Vectors at the leading edge of impeller are parallel to the inlet angle of blades. Thus no reverse flow and flow separation are visible.

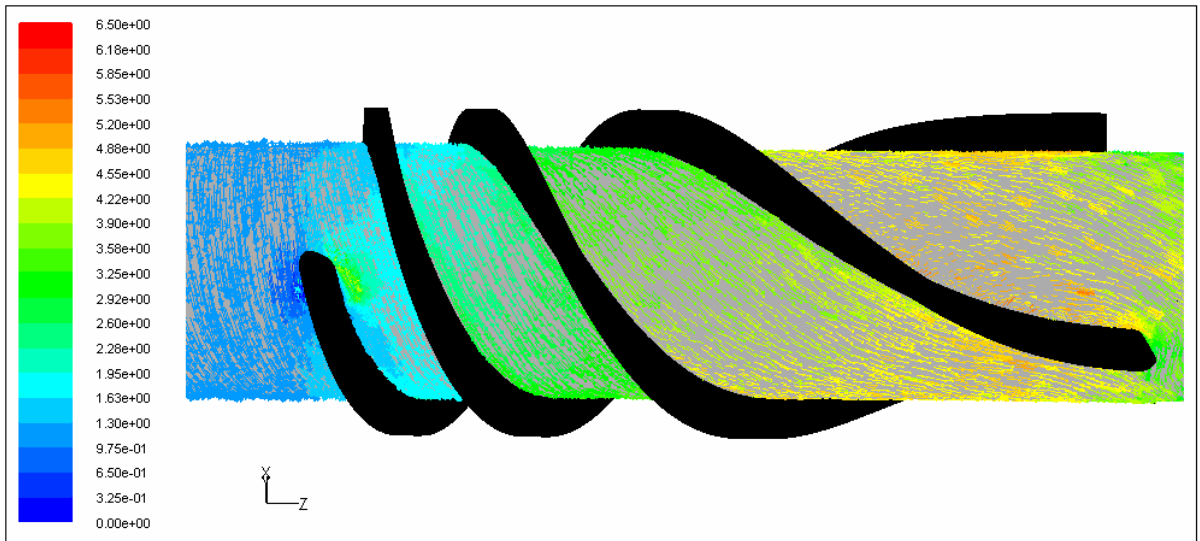


**Figure 3.22: Relative velocity vectors of the arc models impeller**

The distribution of the absolute velocity vectors on the midplane around the diffuser are shown in Figure 3.23. No flow separation is seen at the inlet, but vector distribution is not uniform at the outlet. Velocity vectors are not parallel to the blade. Flow separation occurs at nearly half of the blade length. Flow has a tangential component at the outlet, which is not desired.

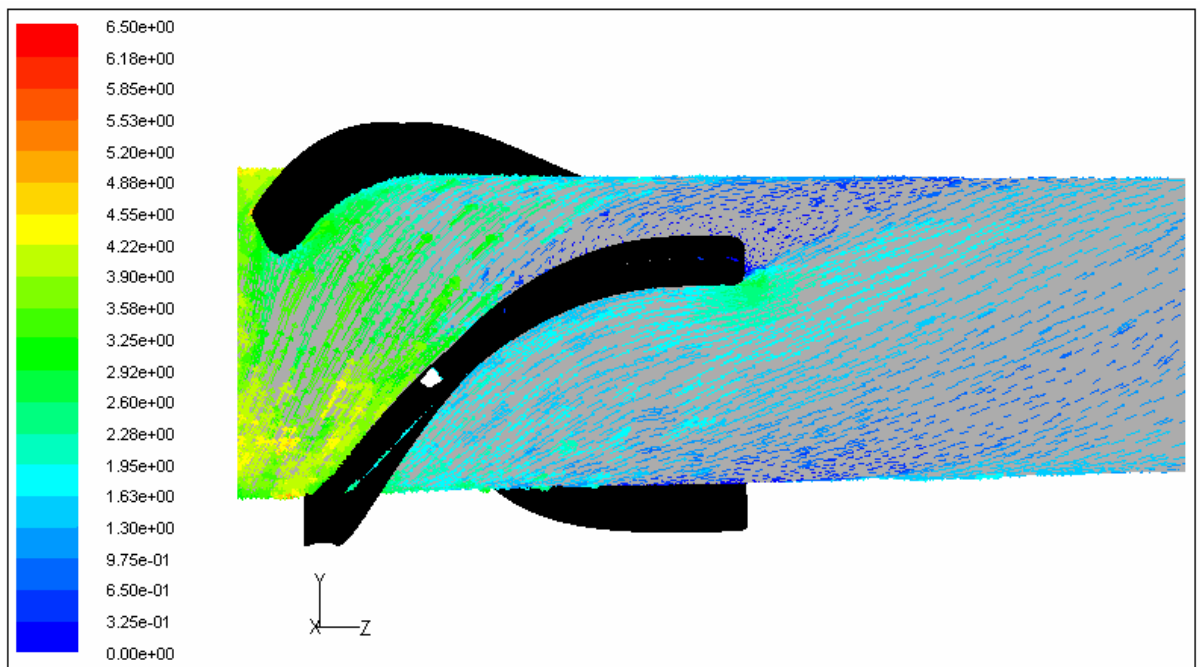


**Figure 3.23: Absolute velocity vectors of arc models diffuser**

## 3.5 Axial Pump With Constant Pressure Increase Through The Blades

It is aimed to design an axial LVAD by using the Euler turbomachinery equation. Blade length in axial direction is divided into ten equal sections. It was aimed that each section generates the same pressure rise. This is also means  $\frac{\Delta P}{\Delta Z}$  is equal for each section.

### 3.5.1 Calculations

Our strategy in this design is dividing the impeller blade into ten equal sections in axial flow direction. Total length of the impeller in axial direction is 27.34 mm and length of each section is decided to be 2.734 mm. We design the blade camber so that each section supplies %10 of total pressure rise which is generated through impeller blades. This means the energy rates transferred per unit mass flow are equal for each section. Hence, the inlet and outlet angles of each section is calculated via Euler turbomachinery equation.

Blade speed is one of the parameters which is essential for blade designing. As seen in formula (5), revolutions per minute and blade radius values are needed to calculate the blade speed. Radius measures can be taken from tip, mean or hub points of blade as shown in Figure 3.24.

The magnitude of blade speed has a great effect on blade inlet angle. Because blade speed is also assumed as the tangential flow velocity at the leading edge of impeller blade. Higher blade speeds means acuter inlet angles for a constant axial flow velocity. As a straightened flow is aimed at the outlet region of impeller blades, the outlet angle is constant and  $90^\circ$  for all designs. Thus if the inlet angle is acuter, the revolution times of blade around the hub would be more to have a  $90^\circ$  of an outlet angle. More number of blade revolutions around the hub is an undesired situation due to the blood damage risk. As a solution, the blade speed is calculated by using the hub radius value to have a fine blade geometry. Blade speed calculation and the velocity values are shown in figure below.

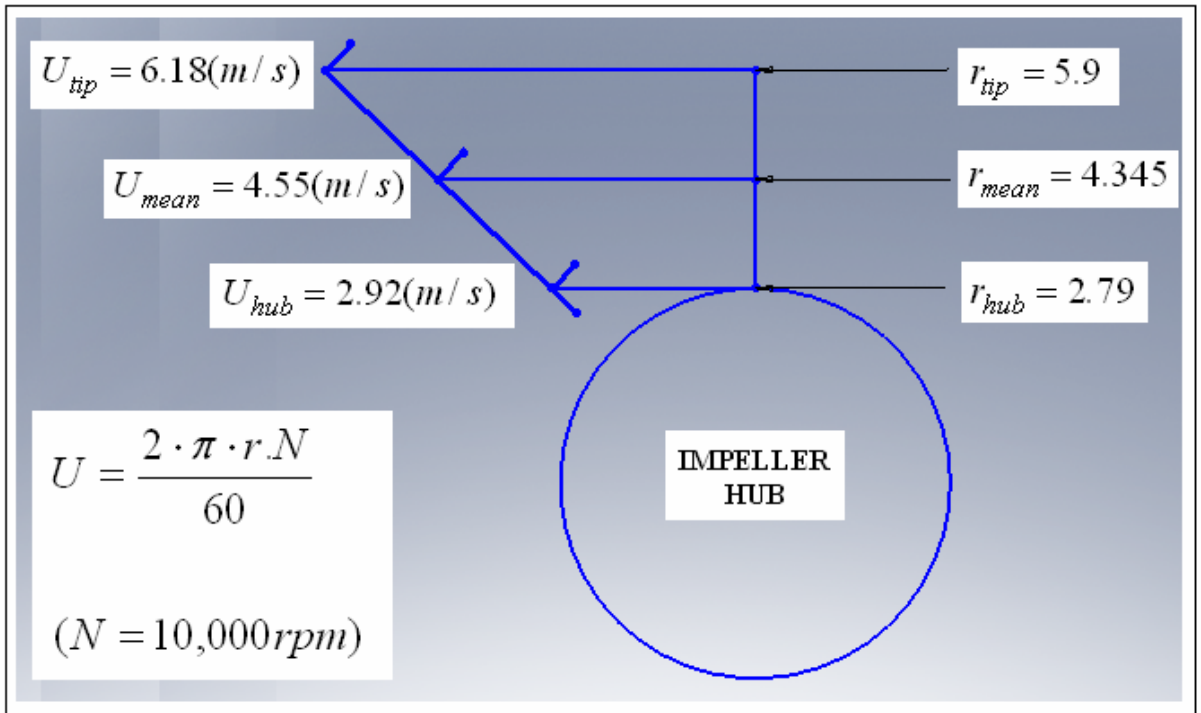


**Figure 3.24: Blade Speed Calculation**

At the first step, rotor speed is calculated from the hub of impeller by using the formula (2.5).

$$U = 2.92 (m / s)$$

Enthalpy change and pressure rise values are also calculated after the rotor speed is found.

$$\Delta H = W = H_1 - H_2 = w \cdot r \cdot (C_{\theta 1} - C_{\theta 2}) = U \cdot (C_{\theta 1} - C_{\theta 2}) \quad (3.2)$$

$$\Delta H = 8.53 (Nm)$$

$$\Delta P = \rho \cdot \Delta H \quad (3.3)$$

$$\Delta P = 8957 (Pa)$$

$$\Delta h = \frac{\Delta H}{10} = 0.853 (Nm)$$

Since a straightened flow is aimed,  $C_{\theta 2}$  is assumed to be zero.  $\rho$  is density of blood which is equal to  $1050 kg / m^3$ .  $\Delta H$  is the total enthalpy change of blood through the



impeller and  $\Delta h$  is the enthalpy change at each sections.  $\Delta P$  is the pressure rise between the inlet and outlet of the impeller. Thus a pressure rise of  $8963Pa$  is expected from the calculations. As mentioned before, the rotor speed can be calculated from three different region on the impeller blade (hub, mean and tip). Both these three velocity values has an effect on the pressure rise magnitudes which are calculated by using the Euler turbomachinery equation. The pressure rise values for different velocities are shown in Table 2.

**Table 2: Pressure difference results for different blade speeds.**

<b>Velocity</b>	<b>(m/s)</b>	<b>Pressure difference</b>	<b>(Pa)</b>
$\underline{U_{hub}}$	2.92	$\underline{\Delta P_{hub}}$	8957
$\underline{U_{mean}}$	4.55	$\underline{\Delta P_{mean}}$	21738
$\underline{U_{tip}}$	6.18	$\underline{\Delta P_{tip}}$	40102

Second step is the calculation of the inlet and outlet angles of each section. Tangential and axial velocity components of flow are needed for this step. As mentioned before axial velocity is constant through the pump. However relative tangential velocities at the inlet and outlet of each sections should be calculated by using Euler turbomachinery equation.

As shown in Figure 3.25, velocity triangles are used in the calculation of inlet and outlet angles.

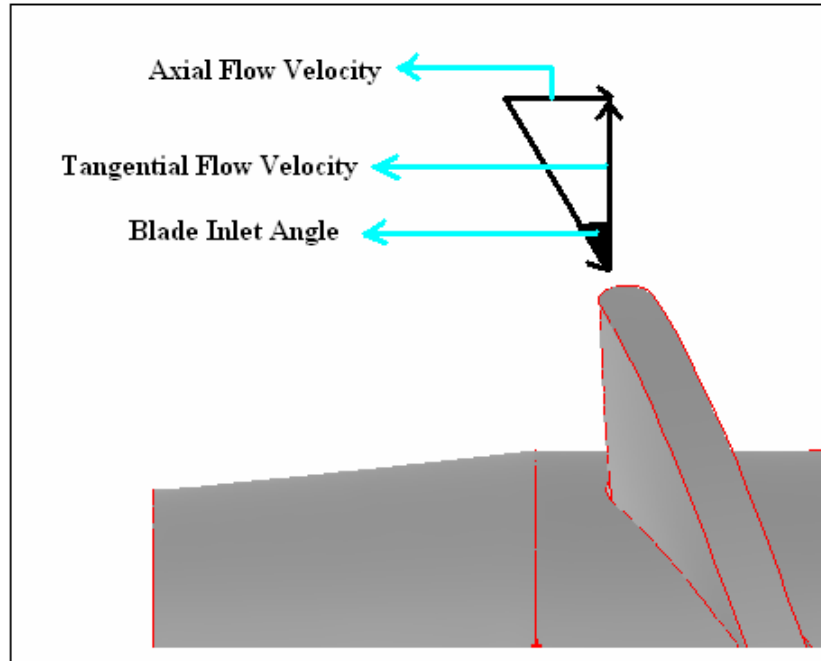


**Figure 3.25: Calculation of the inlet angle**

Mass flow velocity “ $V_a$ ” in axial direction is calculated by using the formula below.

$$\dot{m} = \rho \cdot A \cdot V_a \quad (3.4)$$

$\dot{m}$  is the mass flow rate of blood (6l/min) and  $A$  is the flow area which is vertical to the axial flow direction. Flow area is found by subtracting hub and blade areas from the total inlet area.

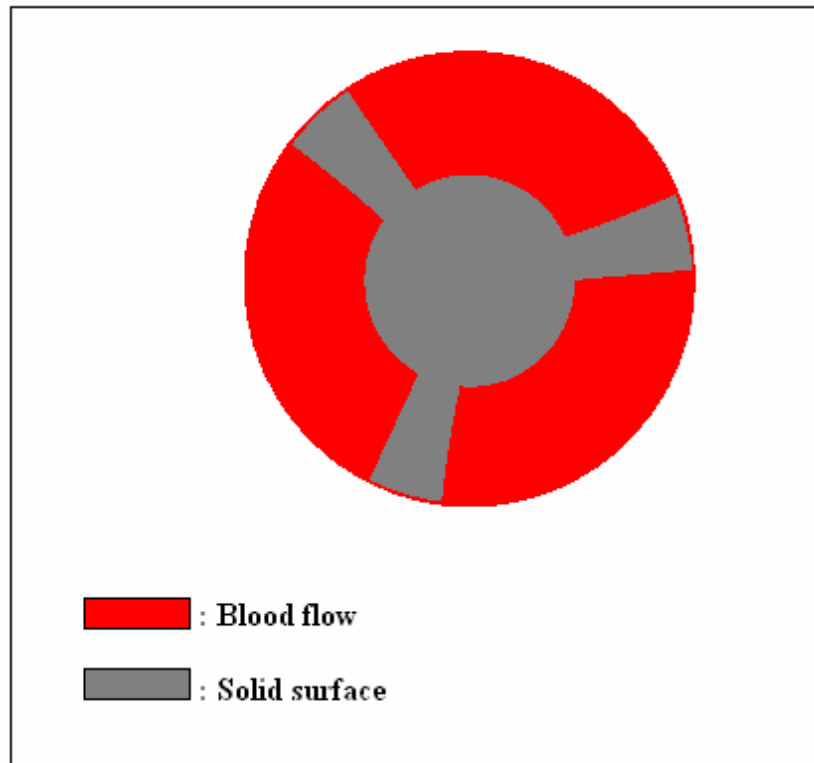


**Figure 3.26: The flow area in axial direction**

$$A = [(\Pi.r_{shroud}^2 - \Pi.r_{hub}^2) - (blade\_area)]$$

$$A = 7.11 \cdot 10^{-5} (m^2)$$

Axial flow velocity is calculated by using the formula (3.4) after the flow area is found.

$$V_a = 1.41 (m/s)$$

As the first section is also the inlet region of the impeller blade, relative tangential velocity is maximum here and equals to the blade speed. Thus there is no need to calculate a relative tangential velocity for the inlet of the first section. By using rotor speed and axial flow velocity, first inlet angle ( $\alpha_1$ ) is calculated as seen below.

$$\alpha_1 = a \tan\left(\frac{C}{U}\right) \quad (3.5)$$

$$\alpha_1 = 25.71^\circ$$

After the first inlet angle was calculated, second sections relative tangential velocity “ $W_{\theta 2}$ ” is calculated. The Euler turbomachinery equation is used also for this calculation.

$$\Delta h = 0.853(Nm)$$

$$W_{\theta 1} = U = 2.92(m/s)$$

By using the formula (3.2),  $W_{\theta 2}$  is calculated.

$$W_{\theta 2} = 2.63(m/s)$$

The outlet angle of the first section is the inlet angle of the second section “ $\alpha_2$ ”. It is calculated by using the same method.

$$V_a = 1.41(m/s)$$

$$U = 2.63(m/s)$$

$$\alpha_2 = a \tan\left(\frac{C}{U}\right) = 28.14^\circ$$

Other inlet and outlet angles are also calculated similarly. As there are 10 sections through the axial direction, 10 inlet and 10 outlet angles are calculated.

**Table 3: Inlet and outlet angles of each section.**

	<b>Inlet Angle (degree)</b>	<b>Outlet Angle (degree)</b>
<b>1. Section</b>	<b>25.71</b>	<b>28.14</b>
<b>2. Section</b>	<b>28.14</b>	<b>31.04</b>
<b>3. Section</b>	<b>31.04</b>	<b>34.52</b>
<b>4. Section</b>	<b>34.52</b>	<b>38.74</b>
<b>5. Section</b>	<b>38.74</b>	<b>43.92</b>
<b>6. Section</b>	<b>43.92</b>	<b>50.28</b>
<b>7. Section</b>	<b>50.28</b>	<b>58.07</b>
<b>8. Section</b>	<b>58.07</b>	<b>67.44</b>
<b>9. Section</b>	<b>67.44</b>	<b>78.27</b>
<b>10. Section</b>	<b>78.27</b>	<b>90</b>

Change of tangential velocity values are listed in Table 4 below. The relative tangential velocity is equal to the blade speed at the inlet of impeller blades. The sum of the relative and absolute tangential velocity values are always constant and equal to the total tangential velocity.

**Table 4: Change of relative and absolute tangential velocities through the sections.**

<b>At the End of</b>	<b>Relative tangential velocity (m/s)</b>	<b>Absolute tangential velocity (m/s)</b>
<b>1. Section</b>	<b>2.63</b>	<b>0.29</b>
<b>2. Section</b>	<b>2.34</b>	<b>0.58</b>
<b>3. Section</b>	<b>2.05</b>	<b>0.88</b>
<b>4. Section</b>	<b>1.75</b>	<b>1.17</b>
<b>5. Section</b>	<b>1.46</b>	<b>1.46</b>
<b>6. Section</b>	<b>1.17</b>	<b>1.75</b>
<b>7. Section</b>	<b>0.88</b>	<b>2.05</b>
<b>8. Section</b>	<b>0.58</b>	<b>2.34</b>
<b>9. Section</b>	<b>0.29</b>	<b>2.63</b>
<b>10. Section</b>	<b>0</b>	<b>2.92</b>

### **3.5.2 Solid Modeling**

After the blade inlet and outlet angles are calculated, the solid model of impeller is created by using Pro Engineer and Solid Works. Dimensions as impeller length, impeller radius, blade length, blade tip radius and shroud radius values are the same with the impeller of MicroMed DeBakey LVAD.

Impeller hub radius = 2.79 mm

Impeller length in axial direction = 34.41 mm

Blade length in axial direction = 27.34 mm

Blade tip radius = 5.9 mm

Shroud radius = 6 mm

Impeller blade length is divided into ten equal sections as mentioned before:

Length of each section in axial direction = 2.734 mm

Solid modeling is started at Pro Engineer with drawing a cylinder which has a radius of 2.79 mm. This cylinder is the hub of impeller. Then a spline is created as shown in Figure 3.28 and wrapped around the hub. All starting and ending points of each section has been designated geometrically by using inlet angle and section lengths in axial direction.

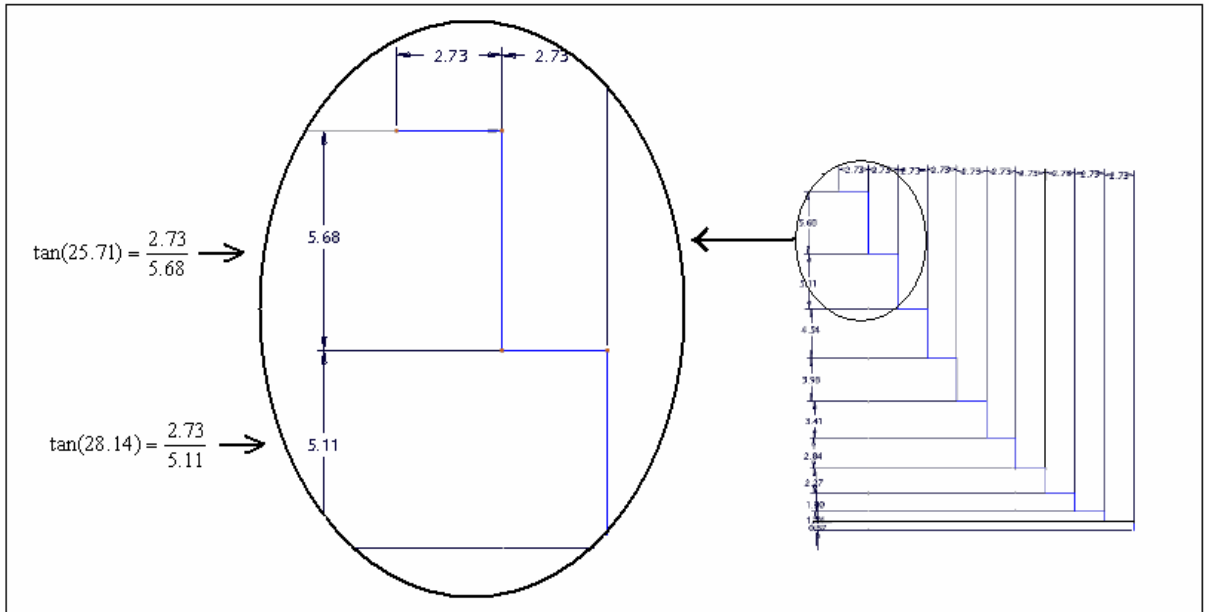


**Figure 3.27: Section lengths in axial and tangential directions.**

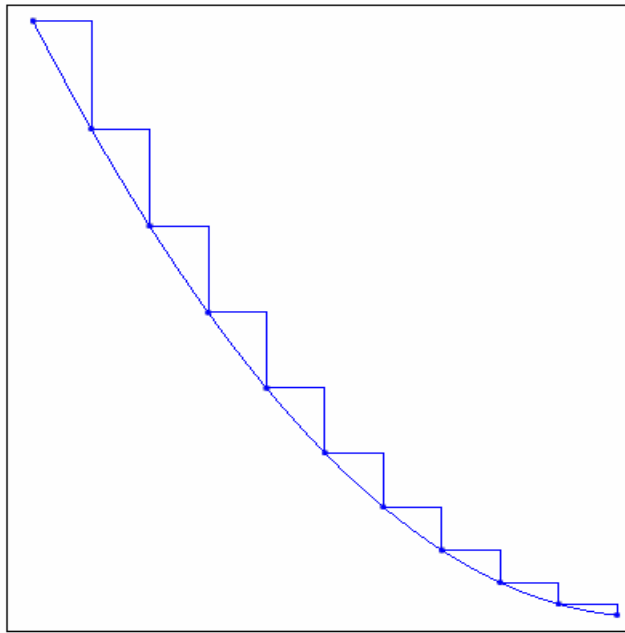


**Figure 3.28: Spline creation.**

After the spline is created, it is wrapped around the cylinder.

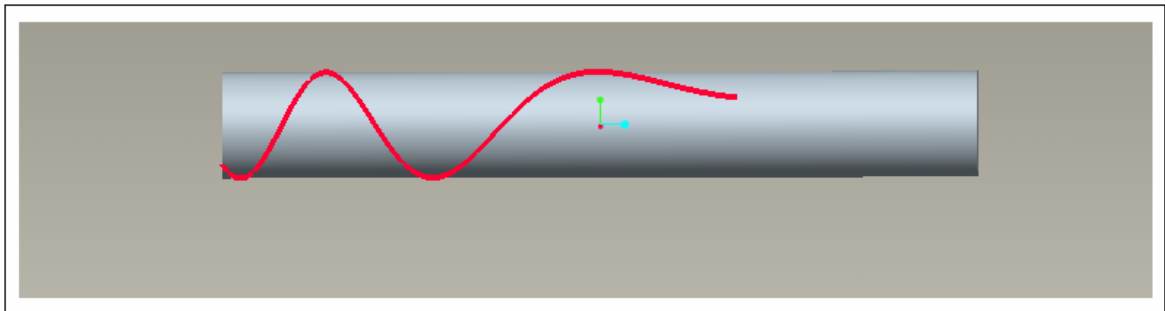


**Figure 3.29: Wrap around the cylinder**

Then one of the blades is created with no thickness. (As shown in Figure 3.30)

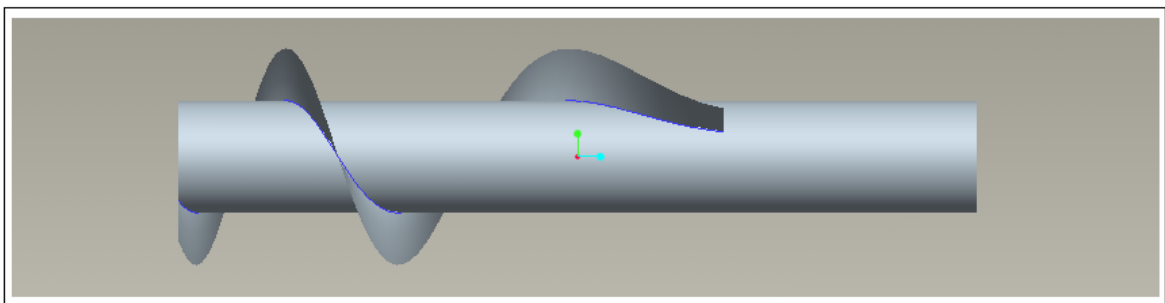


**Figure 3.30: Blade creation by spline**

Other blades are also created with no thickness as seen in Figure 3.31

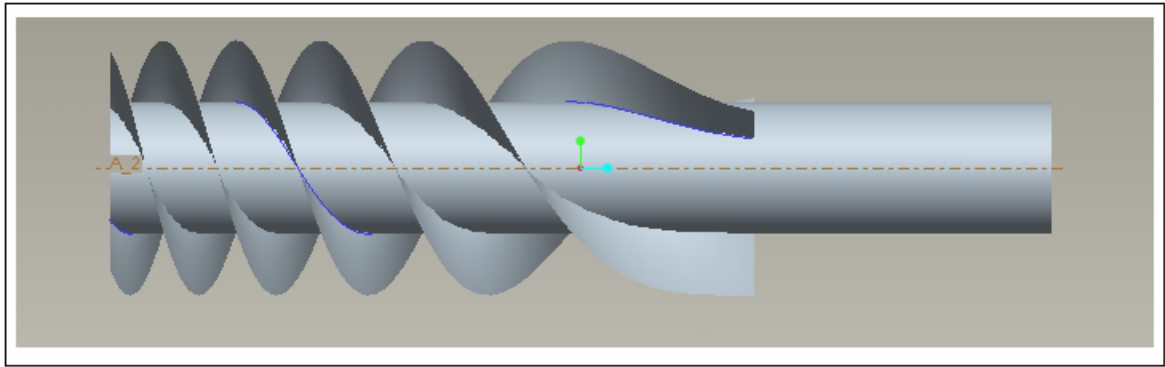


**Figure 3.31: Impeller blades created by spline**

Inspection of the created blade geometry shows that the blades are close to each other especially in the inlet region. This can cause some problems during the blood flow. As mentioned before, our model should ensure a uniform blood flow and transform kinetic energy to enthalpy gradually. There is already a turbulent flow due to the high rotational speed at impeller. If the blade geometry would not be suitable, blood cells can undergo structural changes.

### **3.5.3 Modifications**

The aim is designing a better blade geometry than the geometry which is created by using the Euler turbomachinery equation with equally divided sections in axial direction. At first, the section lengths of the impeller blade in axial direction are examined. As shown in Table 5, lengths of sections in axial direction also has an effect on the blade lengths in tangential direction especially at primary sections. Tangential length means, blade revolutions around the hub of impeller. The design which has equal axial lengths can promise us enough pressure rise in theory, however it is difficult to have a uniform flow with minimum blood damage. Because if the tangential length of blade gets higher, blood will have more revolutions through the impeller hub. This means higher velocities and larger blood damage risk. Thus the axial blade lengths are modified. Especially axial lengths of primary sections are shortened. On the other hand, final sections are lengthened in axial direction to keep the total impeller blade length in axial direction constant.

To insure an axial blood flow at the trailing edge of the impeller, extra straightener sections with 2.5 mm lengths are added to each blade. This extra sections have same inlet and outlet angles which is  $90^\circ$ . The original axial length was kept constant during the modifications.



**Table 5: Blade lengths of modified models**

	<u>Equally Divided</u>		<u>1. Modification</u>		<u>2. Modification</u>		<u>3. Modification</u>	
	<u>Impeller Blade Lengths (mm)</u>							
<u>Section</u>	<u>Axial</u>	<u>Tangential</u>	<u>Axial</u>	<u>Tangential</u>	<u>Axial</u>	<u>Tangential</u>	<u>Axial</u>	<u>Tangential</u>
<u>1</u>	2.734	5.68	0.5	1.04	0.5	1.04	0.5	1.04
<u>2</u>	2.734	5.11	0.5	0.93	0.5	0.93	0.5	0.93
<u>3</u>	2.734	4.54	0.5	0.83	0.5	0.83	0.5	0.83
<u>4</u>	2.734	3.98	0.5	0.73	0.5	0.73	0.5	0.73
<u>5</u>	2.734	3.41	0.5	0.62	0.5	0.62	0.5	0.62
<u>6</u>	2.734	2.84	4.468	4.64	2.23	2.32	2.98	3.09
<u>7</u>	2.734	2.27	4.468	3.71	2.23	1.86	2.98	2.47
<u>8</u>	2.734	1.70	4.468	2.78	2.23	1.39	2.98	1.86
<u>9</u>	2.734	1.14	4.468	1.86	4.47	1.86	2.23	0.93
<u>10</u>	2.734	0.57	4.468	0.93	11.17	2.32	11.17	2.32
<u>Extra</u>	0	0	2.5	0	2.5	0	2.5	0

Solid models of 3 modified impeller geometries are shown below.

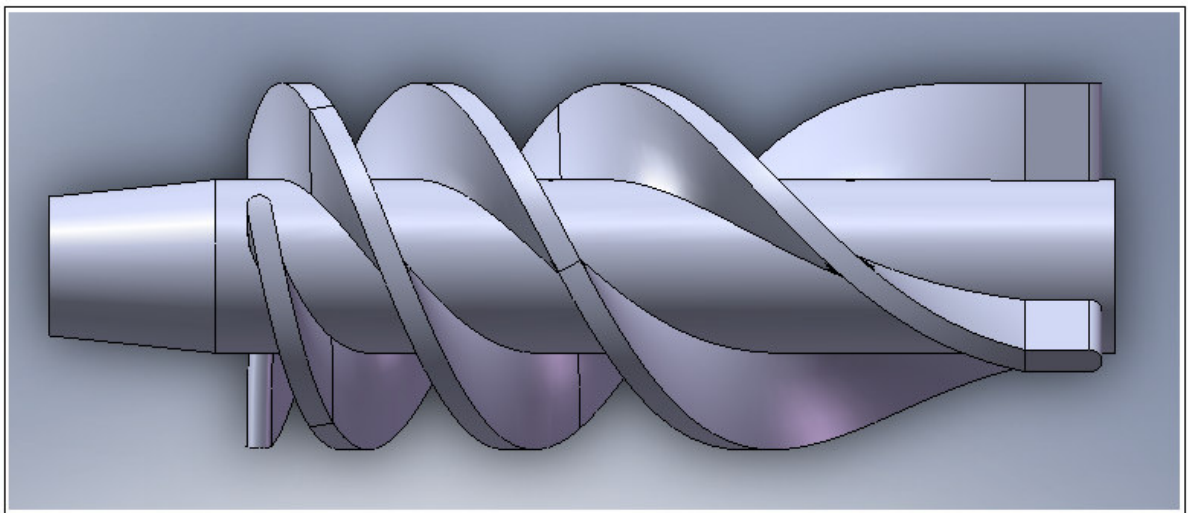


**Figure 3.32: 1. Modification model (impeller)**

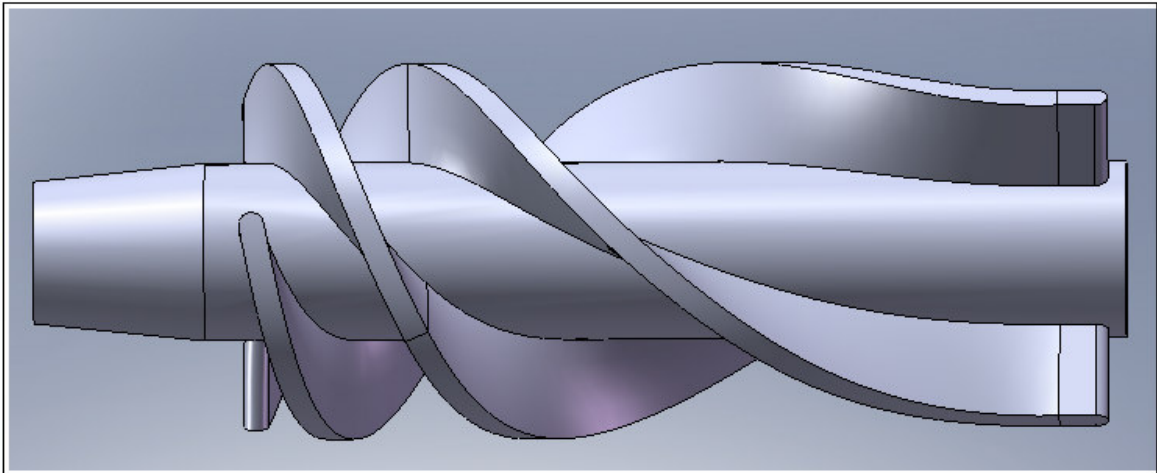


**Figure 3.33: 2. Modification model (impeller)**

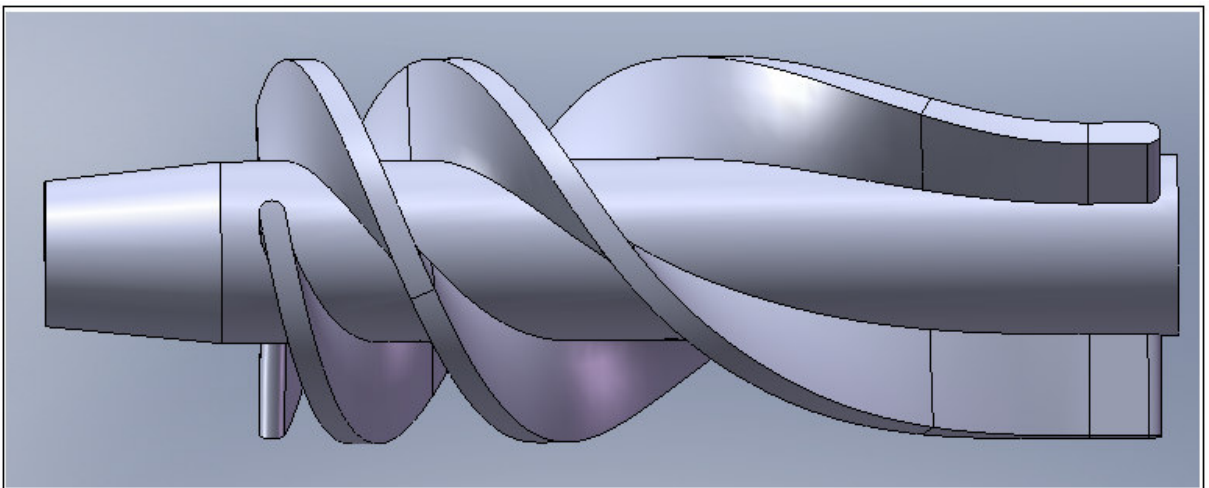


**Figure 3.34: 3. Modification model (impeller)**

### **3.5.4 Simulation Results of Modification Models**

Three different solid geometries are generated after the impeller blade geometries are modified. Same diffuser and inducer models are used in all simulations. The results are compared as shown in the Table 6.

**Table 6: Pressure rises and wall shear stresses**

	Arc Geometry	1.Modification	2.Modification	3.Modification
Pressure Rise (Pa)	10 743	10 480	10 680	10 856
WSS (Pa)	120	120	111	113

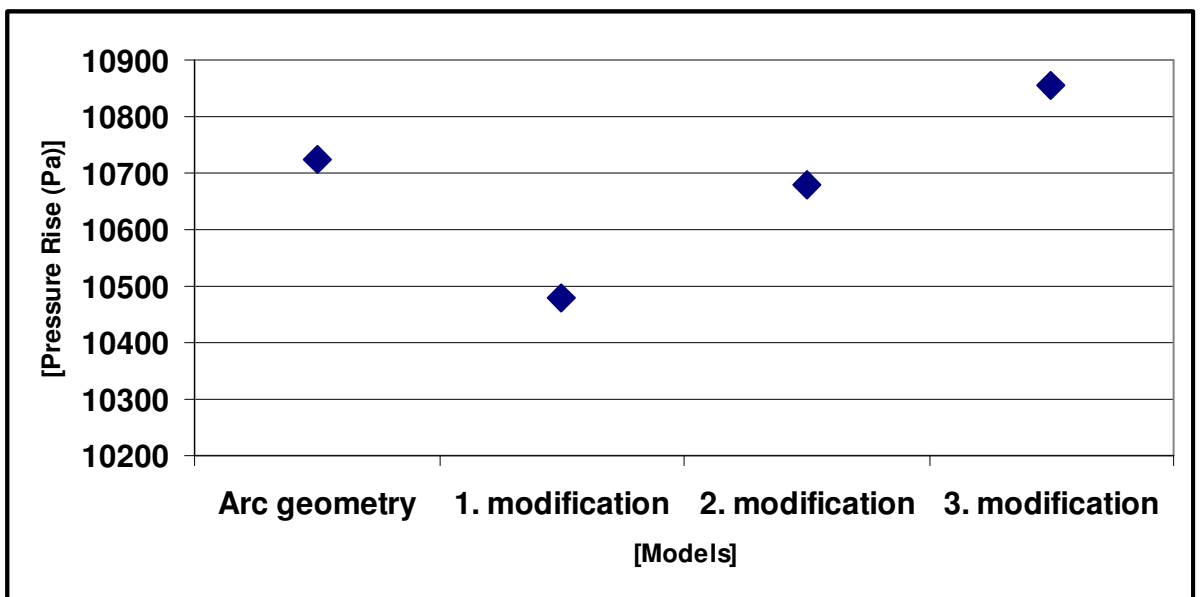


**Figure 3.35: Comparison of pressure rises**

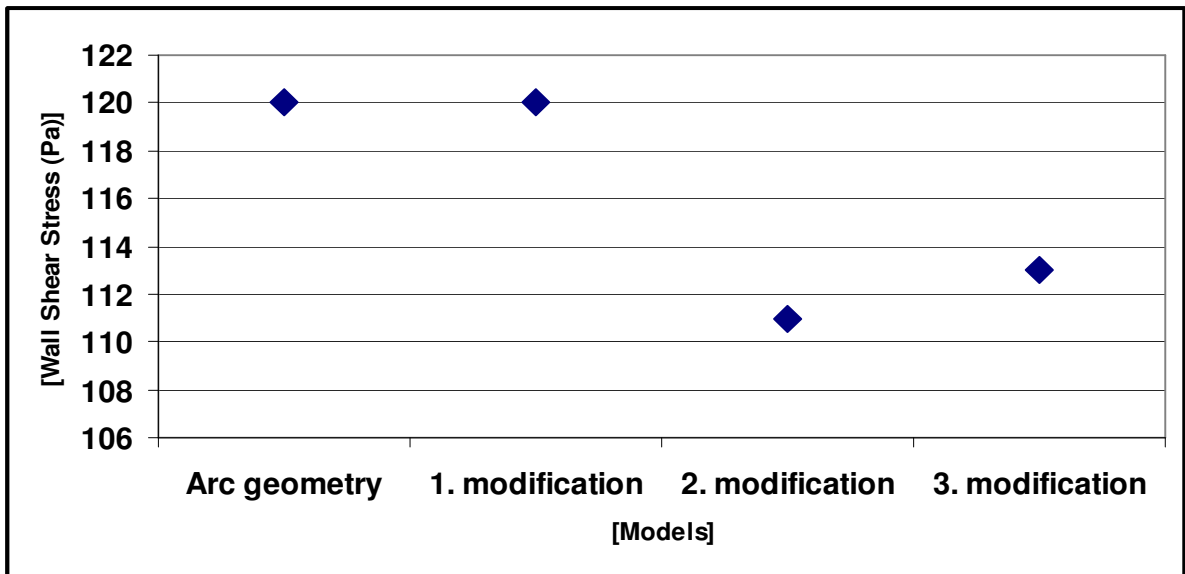


**Figure 3.36: Comparison of wall shear stresses**

Although the pressure rise and WSS results of all four models are close to each other, the 3. modification model gives the highest pressure rise value. Thus the 3. modification model is chosen as the most suitable axial left blood pump model for our study which is designed by using the Euler's turbomachinery equation.

### **3.5.5 Simulation Results of the 3. Modification**

Pressure distribution of the 3. modification model is shown at Figure 3.37. There is a pressure difference of 10 856 Pa between inlet and outlet regions. This value is higher than the arc models pressure rise value.

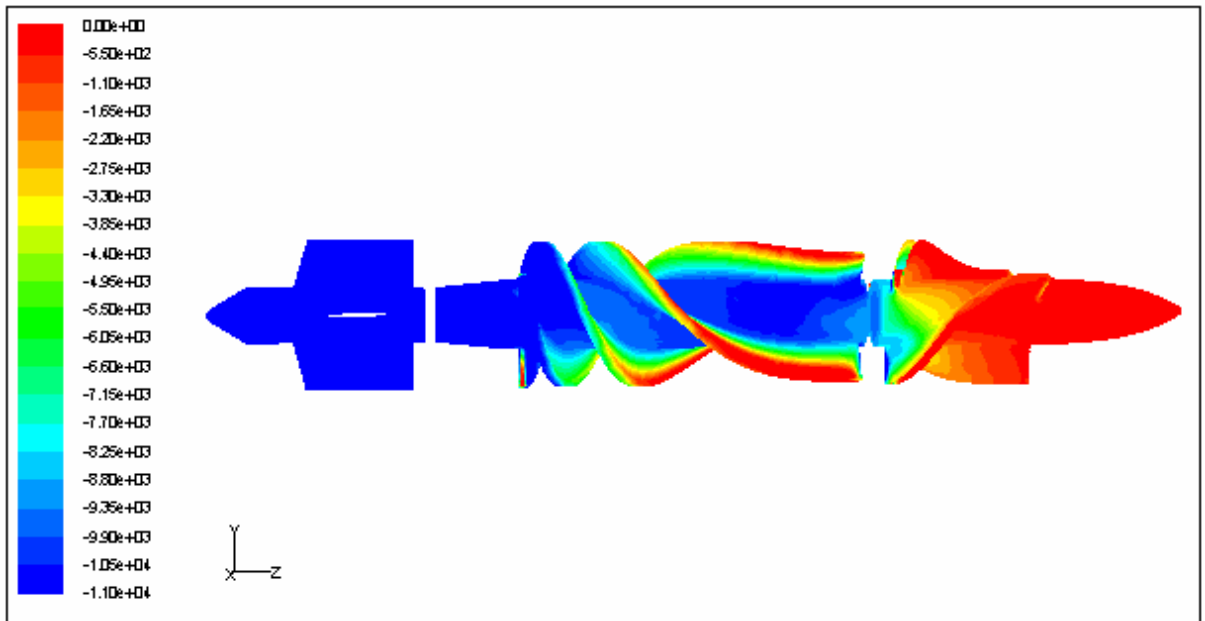


**Figure 3.37: Pressure distribution of the 3. modification**

The average WSS at impeller is 113 Pa for the 3. modification model.

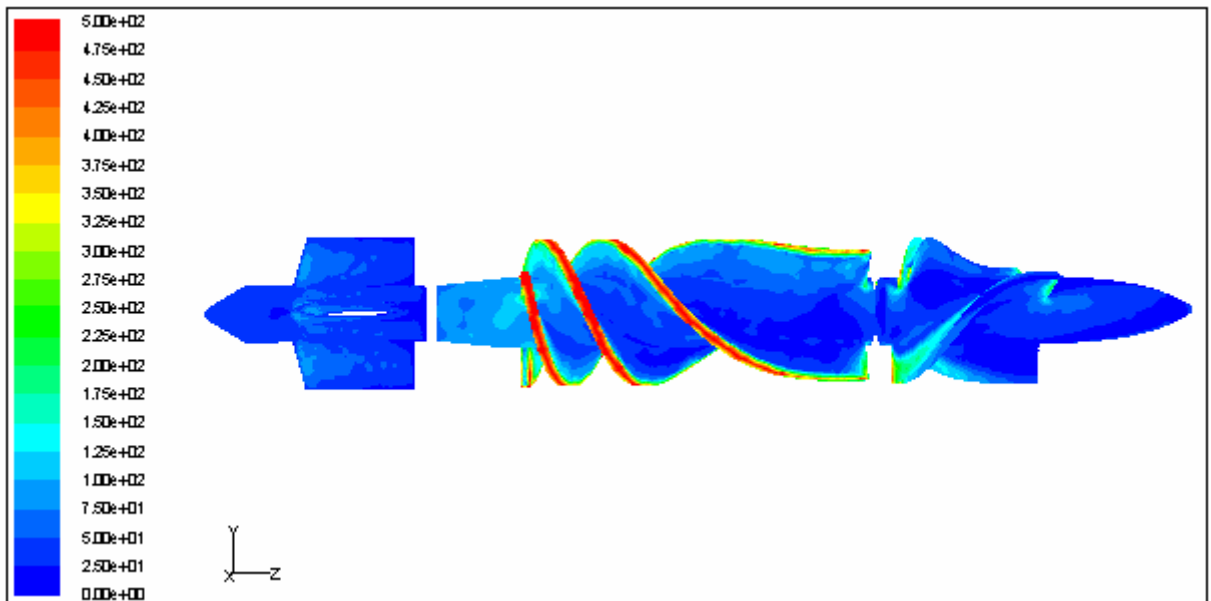


**Figure 3.38: WSS distribution of the 3. modification**

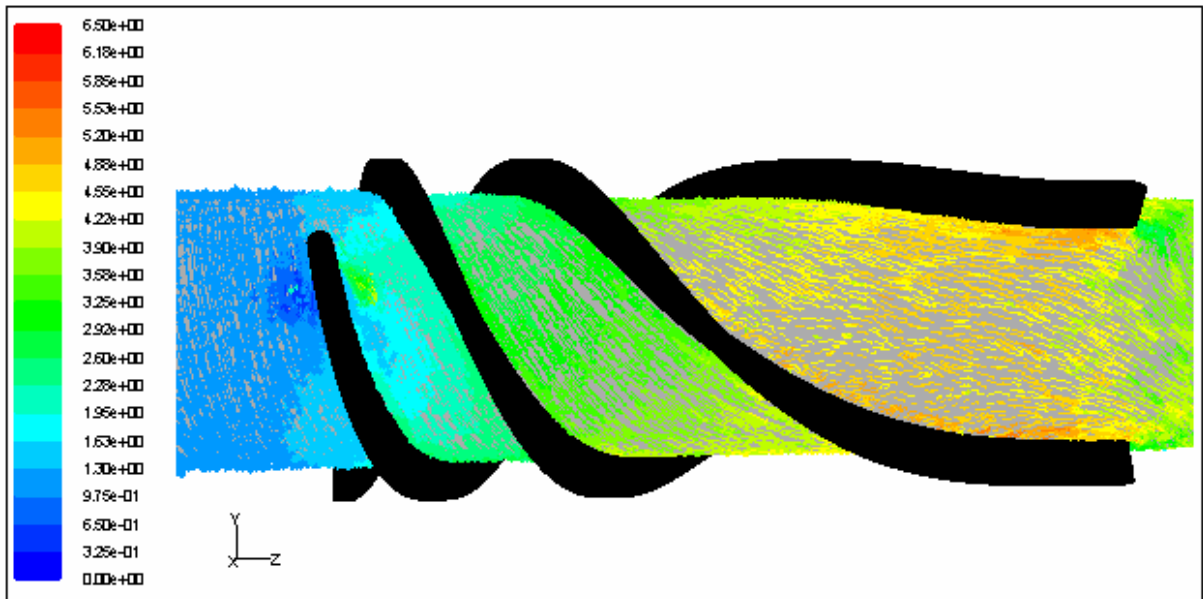


**Figure 3.39: Relative velocity vectors of 3. modification**

### 3.6 Results

Simulation results showed that the size and the directions of relative velocity vectors are dramatically changed when blood is passing through the region which is between the impeller blades and the shroud. Thus the high shear stresses occurred through the tip of impeller blades.

Blade inlet angles and blade geometries of impeller and diffuser parts are only the difference between these four models. Thus the effect of blade geometry on blood flow is investigated. The 3. modification model which is calculated by using both the Euler turbomachinery equation and arcs gave better results than the other models. 10 856 Pa of pressure rise is generated at 3. modification model. 5 868 Pa of total pressure rise was generated at the impeller and 5 837 Pa is generated at the diffuser. There is also a 849 Pa pressure decrease between pump inlet and inducer outlet due to the inducer which is the flow straightener part. Thus the degree of reaction for 3. modification model is:

$$\lambda = \frac{\text{pressure generated through the impeller}}{\text{pressure generated through the pump}} = \frac{5868}{10856} = 0.54$$

The pressure rise and WSS comparisons of four different models are given below. As mentioned before, the highest pressure rise is generated through the 3. modification model for 10 000 rpm and 6 l/min.

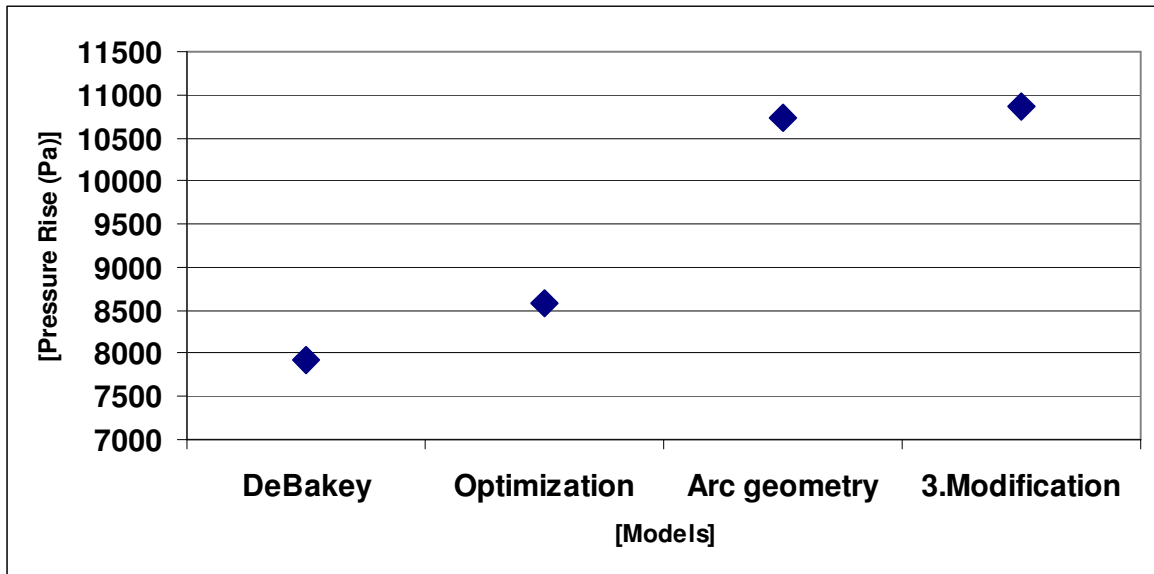


**Figure 3.40: General comparison of pressure rises**

The minimum WSS is generated in the optimization model. However the WSS differences between the models are not so much. Also the values are not at the critical levels. Thus the pressure rise generation is a more important characteristic for these pumps. On the other hand the 3. modification model gives almost same WSS and pressure rise results at 9 300 rpm and 6 l/min. The pressure rise through the MicroMed DeBakey LVAD at 10 000 rpm is also provided by the third modification model at 9 000 rpm.

**Table 7: Pressure rise and WSS levels of 3. modification model at different rpms.**

Rotational Speed (rpm)	Pressure Rise (Pa)	WSS (Pa)
8000	4707	97
9000	7619	105
9300	8554	107

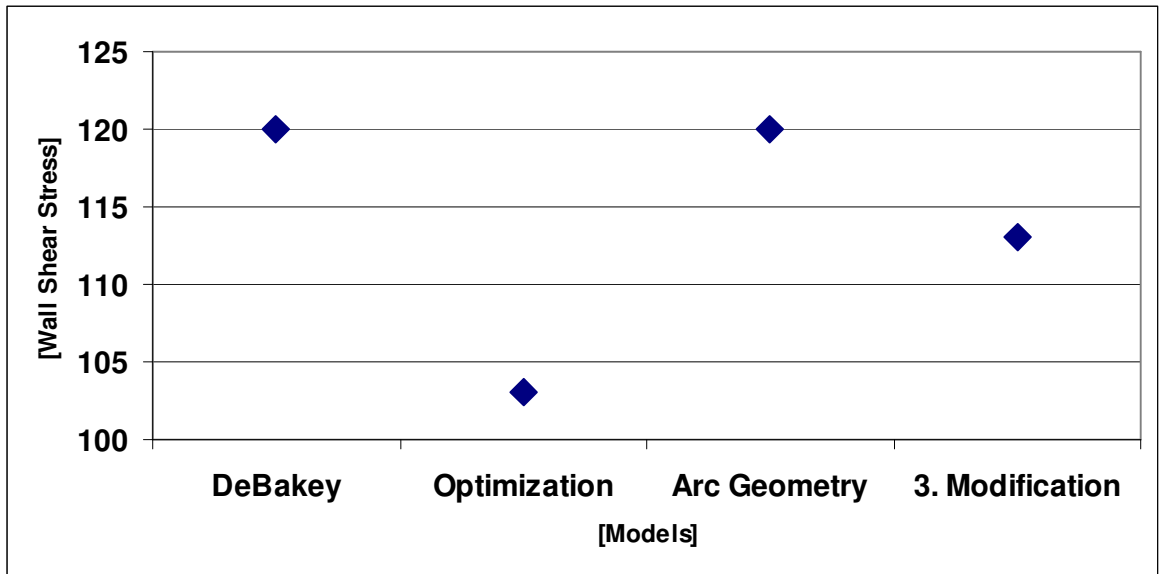


**Figure 3.41: General comparison of WSS**

Characteristic curve of the 3. modification model is shown in the figure below. The curve represents the pressure rise values at 10 000 rpm for five different mass flow rates.

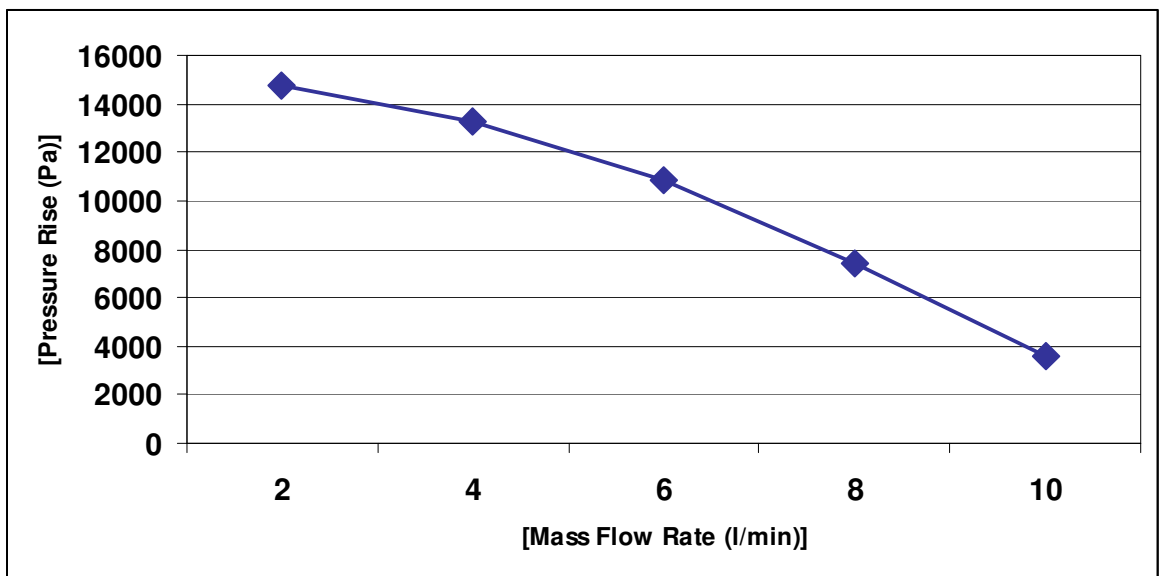


**Figure 3.42: Characteristic curve of the 3. modification model**



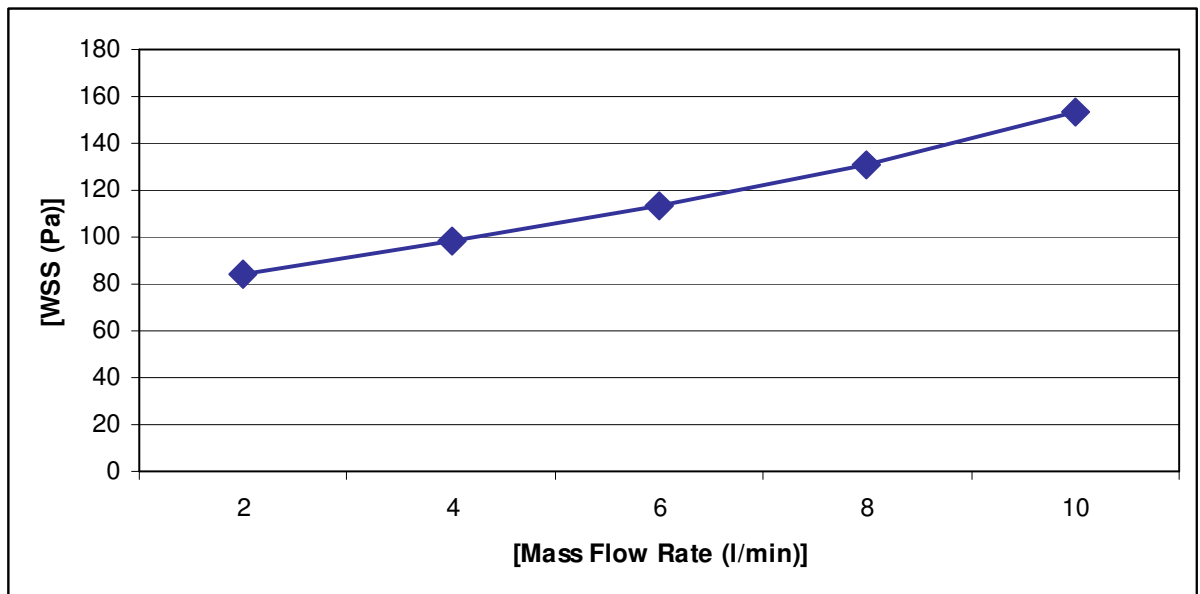


**Figure 3.43: WSS rates of the 3. modification model for different mass flow rates**

## 4 Discussion

In our study it is aimed to provide an optimum blood flow through an axial blood pump. In the beginning the MicroMed DeBakey LVAD model is chosen as the baseline of this study, because it is one of the widely used axial LVADs in the clinical setting. Then three different blood pump models are created via different design methods. By using CFD, blood flow in these four different axial pumps are investigated and the results are compared.

The first investigated model is the MicroMed DeBakey LVAD which is one of the mostly preferred axial blood pumps in the clinical setting. MicroMed DeBakey LVAD is also chosen as the baseline geometry of this study. Then an optimization model which is generated via a parametric design method was also investigated. The number of blades at the impeller and the diffuser of optimization model is same with the MicroMed DeBakey LVAD's. Although better results are provided by the optimization model, the geometries are limited by the limits of the geometrical parameters. Thus a different design method was chosen at the third design and an axial pump was generated with arc shaped blades. The impeller of the third model has no splitter blades and there are three blades at the diffuser of the third model. At the fourth design, the blades are divided into ten equal sections in

axial direction. It is aimed to provide constant pressure rise at the each sections. The calculations are done by using the Euler turbomachinery equation and the geometry is generated. As the distance between the blades were close to each other, the section lengths in axial direction are modified and a better geometry is generated. Finally there is no splitter blades at the fourth design and the number of diffuser blades is three.

After the designs are numerically investigated, the results are compared as shown in Figure 3.40 and Figure 3.41. The simulation results show that the sectioned model provides a %38 higher pressure rise with a %6 lower wall shear stress level than the MicroMed DeBakey LVAD.

The aim of this study was optimizing the blood flow through a LVAD. Finally the sectioned model provided higher pressure rise with an acceptable blood damage rate than the other three models.

## REFERENCES

1. Chua, L. P., Su, B., Lim, T. M., Zhou, T., 2007, "Numerical Simulation of an Axial Blood Pump", *Artificial Organs*, Vol. 31, 560-570
2. Triep, M., Brücker, C., Schröder, W., Siess, T., 2006, "Computational Fluid Dynamics and Digital Particle Image Velocimetry Study of the Flow Through an Optimized Micro-axial Blood Pump", *Artificial Organs*, Vol. 30, 384-391
3. Mitoh, A., Yano, T., Sekine, K., Mitamura, Y., Okamoto, E., Kim, D. W., Yozu, R., Kawada, S., 2003, "Computational Fluid Dynamics Analysis of an Intra-Cardiac Axial Flow Pump", *Artificial Organs*, Vol. 27, 34-40
4. Zhang, Y., Xue, S., Gui, X., Sun, H., Zhang, H., Zhu, X., Hu, S. S., 2006, "A Novel Integrated Rotor of Axial Blood Flow Pump Designed With Computational Fluid Dynamics" *Artificial Organs*, Vol. 31, 2007
5. Untaroiu, A., Throckmorton A. L., Patel, S. M., Wood, H. G., Allaire, P. E., Olsen D. B., 2005, "Numerical and Experimental Analysis of an Axial Flow Left Ventricular Assist Device: The Influence of the Diffuser on Overall Pump Performance" 2005, *Artificial Organs*, Vol., 581-591
6. Song, X., Untaroiu, A., Wood, H. G., Allaire, P. E., Throckmorton, A. L., Day, S. W., Olsen, D. B., 2004, "Design and Transient Computational Fluid Dynamics Study of a Continuous Axial Flow Ventricular Assist Device", *ASAIO Journal*
7. Anai, H., Wakisaka, Y., Nakatani, T., Taenaka, Y., Takano, H., Hadama, T., 1996, "Relationship Between Pump Speed Design and Hemolysis in an Axial Flow Blood Pump" *Artificial Organs*, Vol. 20, 564-567
8. Kwant, P.B., *Implantable electromechanical displacement blood pumps: systematic design and validation methods*, Phd Thesis, RWTH Aachen University, Aachen, 2007
9. Snarnicki, R., "Arterial Disease." Available on site <http://users.rcn.com/szarnick/artery.html>
10. Cohn, L. H., *Cardiac Surgery in the Adult*, Third Edition, McGraw-Hill, New York, 2008
11. Gray, N. A., Selzman C.H. 2006, "Current Status of the Total Artificial Heart", *American Heart Journal*, Vol. 152, 4-10

12. Reul, H. M., Akdis, M., 2000, "Blood Pumps for Circulatory Support", *Perfusion*, Vol. 15, 295-311
13. Gorla, R. S. R., Khan A. A., *Turbomachinery Design and Theory*, Marcel Dekker, New York, 2003
14. Karl, T. R., Horton, S. B., Brizard, C., 2006, "Postoperative Support With the Centrifugal Pump Ventricular Assist Device (VAD)" *Pediatric Cardiac Surgery Annual*
15. Yu, S. C. M., Ng, B. T. H, Chan, W. K., Chua, L. P., 2000, "The flow patterns within the impeller passages of a centrifugal blood pump model."
16. Japikse, D., Baines, N. C., *Introduction to Turbomachinery*, Concepts ETI, Inc. And Oxford University Pres, 1997
17. Sorguven, E., Akgun, M. A., Ahn, H., Ciblak, N., Egrican, A. N., Lazoglu, I., Okyar, A. F., Safak, K. K., Kucukaksu, S., 2007, "Flow simulation and optimization of a left ventricular assist device." *IMECE2007*
18. Ozsoy, B., *Optimization of the Mechanical Performance of an Axial Heart Pump Based on a Parametric Model*, A Graduation Project Report, Yeditepe University, Istanbul, 2007
19. Anderson, J. B., Wood, H. G., Allaire, P. E., Bearnson, G, Khanwilkar, P., 2000, "Computational flow study of the continuous flow ventricular assist device, prototype number 3 blood pump.", *Artificial Organs*, Vol. 24, 377-385

**ÖZGEÇMİŞ**  
**A. Serhan HAKKOYMAZ**

**Kişisel Bilgiler :**

Doğum Tarihi	09.08.1983
Doğum Yeri	Osmaniye
Medeni Durumu:	Bekar

**Eğitim :**

Lise	1998–2001	Adana Anadolu Lisesi
Lisans	2001–2006	Yıldız Teknik Üniversitesi Makine Fakültesi, Makine Mühendisliği Bölümü
Yüksek Lisans	2007-2008	Yeditepe Üniversitesi Fen Bilimleri Enstitüsü, Makine Mühendisliği Yüksek Lisans Programı

**Çalıştığı Kurumlar:**

2006-2007 HSK Havalandırma Endüstri Sanayii ve Ticaret Ltd. Şti  
2007-2008 Yeditepe Üniversitesi Makine Mühendisliği Bölümü (Proje Asistanlığı)